On the thermal performance of naturally ventilated room with straw insulation retrofitted envelope for different climatic zones of India

Karthik A. Sabapathy, Sateesh Gedupudi*

Heat Transfer and Thermal Power Lab, Department of Mechanical Engineering, Indian Institute of Technology Madras, Chennai - 600036, India

Abstract

The heat insulating potential of straw, an agricultural residue, used as part of the envelope of unconditioned buildings is the focus of the current work. Using a CFD software with experimentally validated boundary conditions, transient thermal analysis is performed on a 3-D model room of dimensions 3 m × 3 m × 2.5 m with vents and heat source representing a naturally ventilated indoor space. The thermal performances of a reference uninsulated concrete envelope and a straw insulation-based envelope are compared in terms of quantitative parameters such as indoor air temperature, decrement factor, and time lag as well as a qualitative discussion on the need for occupant adaptation, namely closing or opening of inlet vent and requirement of additional heating. The assessment and subsequent recommendation of straw insulation utilization is done for representative summer and winter days of the five different climatic zones of India. A maximum reduction of up to 3.5

*Corresponding author

Email addresses: aksabapathy@outlook.com (Karthik A. Sabapathy), sateeshg@iitm.ac.in (Sateesh Gedupudi)

June 13, 2021

°C in the peak indoor air temperature is achievable with inlet temporarily closed when straw insulation is included in the envelope in summer conditions. In winter conditions of cold climatic zone, with inlet always closed, use of straw insulation leads to the lessening of additional active heat source requirement by as much as 600 W for the considered model room. Further, the effects of increased straw insulation thickness, removal of heat source, varying inlet air velocity, and changing the position of the straw insulation to the outside are also analysed for the extreme warm and cold conditions.
Keywords: Building envelope, CFD, Natural ventilation, Straw insulation, Transient simulations, Thermal comfort

Nomenclature

c	specific heat (J/kgK).
d	thickness of the envelope (m).
DF	decrement factor.
h	heat transfer coefficient (W/m^{2}K).
I_b	direct/beam component of the total irradiance on a surface (W/m^2).
I_d	diffuse component of the total irradiance on a surface (W/m^2).
I_g	irradiance on a horizontal surface which is equal to the Global Horizontal Irradiance (GHI) (W/m^2).
I_t	total irradiance on a tilted surface (W/m^2).
k	thermal conductivity (W/mK).
q	heat flux (W/m^2).
Q	heat transfer rate (W).
ΔR	difference in the longwave radiation emitted and recived by a surface (W/m^2).
R_b	ratio of the beam radiation on the tilted surface to that on the horizontal surface.
R_f	roughness factor.
t	time (s).
T	temperature (K).

TL	time lag (s).
v	air velocity (m/s).
V_w	velocity of wind specified in weather station data (m/s).
z	height of room (m).
Z	standard wind velocity measurement height (m).

Greek symbols

α_s	absorptivity of a surface.
ϵ_s	emissivity of a surface.
θ_z	zenith angle (°).
ρ	density (kg/m^3).
ρ_g	ground reflectance.
ϕ	tilt angle of a surface (°).

Subscripts

C	concrete.
$conv$	convection.
i	inside surface.
in	indoor.
o	outside surface.
out	outdoor.
P	plaster.

rad	radiation.
S	straw.
sol	sol-air.
$surf$	surface.

Abbreviations

ASHRAE	American Society of Heating, Refrigerating and Air-Conditioning Engineers.
CFD	Computational Fluid Dynamics.
DHI	Diffuse Horizontal Irradiance.
DNI	Direct Normal Irradiance.
ECBC	Energy Conservation Building Code.
GHI	Global Horizontal Irradiance.
NSRDB	National Solar Radiation Database.

1. Introduction

India is facing two closely intertwined challenges of growing housing demand [1] and persistent portion of consumed energy derived from fossil fuels [2]. With the building sector estimated to be contributing to 39% of carbon emissions globally [3], burgeoning built-up area in India does not do any favour in her efforts to fight the consequences of climate change. During the lifetime of a building, considerable energy is used up in maintaining thermally comfortable conditions [4]. An individual accustomed to a conditioned space eventually begins to feel comfortable over a narrow range of thermal conditions [5]. Such a perception of a narrow comfort range, achievable only through active space-conditioning, also plays a role in driving up energy consumption in buildings. To slow down this vicious cycle, innovations aimed at optimizing energy use in buildings are urgently needed. In this regard, passive techniques are worth exploring because of their inherent energy saving potential. One of the simple and cost-effective passive techniques is the introduction of insulation materials [6], of sustainable nature, in the building envelope. Apart from air-conditioned buildings, there are also many buildings still functioning under natural ventilation or mixed-mode ventilation. A significant portion of building occupants in India are dependent on natural/mechanical ventilation or other forms of adaptation to maintain comfort conditions [7]. So, to assess the feasibility of adopting building insulation for unconditioned spaces, more research is necessary to gain better understanding of the effect of insulation on the indoor thermal environment. Energy savings, even to a small degree, can prove beneficial as sustainable bio-based insulation materials are locally sourced and available at exceptionally low cost.

Straw is an agricultural residue generated during the harvest of a number of staple food crops such as rice, wheat, barley, and oat. Straw in the form of rectangular bales were known to be used in load-bearing walls of houses as early as in 1908 in Nebraska, U.S. [8]. The large thickness of such bales (between 35 and 50 cm) ensured excellent thermal insulation. The insulation characteristics of straw was given scientific authenticity when McCabe [9] measured the thermal resistance (R-value) of straw bales for the first time in 1993. Since then, there has been a growing interest in the various characteristics of straw: thermophysical, structural, hygroscopic, sound, and fire resistance [10][11]. Studies involving straw-based prototype buildings have showed that a fastidious design with proper plastering and sealing can ensure minimum moisture related damage to the straw present in the building envelope [12]. In India, it was reported that the annual production of crop residue from 2010 to 2014 was around 521 million tonnes (Mt) with rice and wheat accounting for 121 Mt and 114 Mt, respectively [13]. Kumar et al. [14] reports that 81% of rice stubble and 48% of the wheat stubble are burnt causing pollution in neighbouring towns and cities [15]. The problem of agriculture residue burning is not unique to India as this practice has also been reported in other countries with sizeable agricultural output such as Brazil [16] and China [17]. Converting the waste straw into a construction material can offer an alternative to farmers who are currently left with no choice but to burn the straw in preparation of the land for the next crop cycle.

Table 1: Summary of literature with experimental results of thermal performance of straw buildings.

Work	Building type & location	Envelope configuration	Ambient conditions	Key results
Sabapathy and Gedupudi [18] (2020)	Experiment on straw test room in Chennai, India	Straw cells of 10 cm thickness supported by plywood frame	10-day monitoring period in warm conditions (maximum outdoor air temperature reaching up to 43 °C)	Indoor air temperature as much as 4 °C lower than outdoor air temperature
Marques et al. [19] (2020)	Analytical	Straw bale of thickness between 200 and 500 mm protected by lime mortar/gypsum plasterboard/oriented straw board	Sinusoidal temperature input for 24 hours with fluctuation of 10 °C	Time lag (thermal delay) increasing from about 12 hours to 32.5 hours with increasing thickness
Gallegos-Ortega et al. [20] (2017)	Experiment on straw bale building in Tecate, Baja California, Mexico	400 mm straw bale envelope with 25 mm earth plaster on both sides and supported by wooden beams	73-day monitoring period with outdoor air and outside surface temperatures in the range of 8 °C to 30 °C and 12 °C to 50 °C, respectively	The indoor air and inside surface temperature fluctuations were only about 4°C and 2 °C, respectively
Douzane et al. [21] (2016)	Experiment on straw bale building (2 floors house) in Voyennes, France	440 mm straw bales with 40 mm thick lime plaster and supported by wooden frame	400-day monitoring with outdoor air temperature extremes of 40 °C in summer and -10 °C in winter	Stable indoor temperature ranging between 20 °C and 25 °C maintained
Lee and Yeom [22] (2015)	Experiment on straw bale mock-up room	450 mm thick straw bales with 30 mm plaster and timber support structure	169-day monitoring period across three seasons with outdoor temperature ranging between -10 °C °C and 35 °C	Indoor air temperature variation 11 °C lower than the same in outdoor air temperature during winter. Indoor conditions similar to outdoor during summer
Verbeeck and Ponet [23] (2012)	Experiment on three rooms of a straw bale house in Limburg, Belgium	Straw bale envelope with overall mean thermal transmittance of 0.26 W/m^{2}K	294-day monitoring period covering summer (maximum outdoor temperature of 35 °C) and winter (minimum outdoor temperature of -2 °C) seasons	Maximum indoor temperature 5 °C lower than outdoor in summer and minimum indoor temperature 6 °C higher than outdoor in winter
Wall et al. [24] (2012)	Experiment on prototype house ('BaleHaus') located in University of Bath, U.K.	Prefabricated panels made of 490 mm thick straw bales with 30-35 mm line render and softwood timber support	Year-long monitoring period. Indoor heating for one day to assess heat loss performance	Thermal imaging of building envelope showed no indications of thermal bridging or building defects
Garas and Allam [25] (2011)	Experiment on prototype straw bale building in New Cairo City, Egypt	450 mm straw bales with 50 mm plaster coating	12-day monitoring period with difference in maximum and minimum of wall outside surface temperatures ranging between 20 °C and 33 °C	Difference in maximum and minimum of wall inside surface temperatures ranged between 3 °C and 5 °C only

Table 1: Summary of literature with experimental results of thermal performance of straw buildings.

Work	**Building type & location**	**Envelope configuration**	**Ambient conditions**	**Key results**
Ashour et al. [26] (2011)	Experiment on straw bale house with multiple rooms in Bavaria, Germany	450 mm straw infill within wooden frames and 20 mm plaster coating	261-hour monitoring period with outside surface temperature fluctuation over 24 hours as much as 16 °C	Over 24 hours, inside surface temperature fluctuation does not exceed 5 °C
Holzhueter and Itonaga [27] (2010)	Experiment on milk processing plant with straw envelope located in Kyotango City, Kyoto, Japan	Straw bales with earthen plaster supported by post and beam wooden structure	11-month monitoring period with mean monthly outdoor temperature varying between 4 °C and 26 °C	The mean monthly indoor temperature varied between 15 °C and 26 °C
Whitman et al. [28] (2010)	Simulation	360 mm straw bales with 30 mm earth render	Representative summer (outdoor temperature between 10 °C and 35 °C) and winter (outdoor temperature between -6 °C and 13 °C) days	Indoor temperature for summer between 23 °C and 28 °C and for winter between 7 °C and 14 °C
Elias-Ozkan et al. [29] (2006)	Experiment on straw bale house in Yozgat, Turkey	Envelope made of straw bales	40-day monitoring without internal heating followed by 21-day monitoring with intermittent heating	Results presented for 3 days without heating show significant smoothening of indoor temperature. With heating, straw bale provide better insulation

1.1. *Review of literature*

The following literature review briefly covers the three topics of interest in the current work: (i) thermal performance of straw based constructions, (ii) passive technique of using building insulation materials in the envelope as well as thermal comfort, in the context of Indian climates, and (iii) some of the transient numerical studies carried out on indoor spaces under different ventilation conditions.

1.1.1. *Straw building thermal performance*

Several researchers have opted for experimental approach involving test rooms or case study buildings to assess the performance of straw insulation. Various attributes of straw buildings namely structural [26], moisture infiltration [30][31][32], fire, and sound resistance [24][19][33] have been explored. Here, the focus is on literature discussing the indoor thermal performance. The studies pertaining to thermal performance of straw envelope are summarized in table 1. With the exception of the study by Sabapathy and Gedupudi [18], the test room or buildings considered in these had the following common features: (a) the envelope consisted of straw of large thickness (>20 cm) in the form of bales/panels or as part of a composite wall, (b) the straw wall forms the load-bearing component of the building envelope, and (c) the straw surface is protected by a coating of some type of plaster. The ability of the thick straw bales to inhibit heat transfer and maintain stable indoor environment is evident from the studies. So naturally, to take advantage of the insulation potential, other methods of incorporating straw into the building envelope were explored. Filling hollow concrete blocks [34][35] or clay hollow bricks [36] with straw, mixing straw with clay [37][38][39] or with sand-concrete [40] or with earthen bricks [41] and fabricating high density straw boards [42] were some of the innovations found in literature. All of these require additional processing and manufacturing stages.

A simple and cost-effective way of using straw insulation in buildings is through a retrofitting technique in which straw in the form of non-load bearing compacted cells of smaller thicknesses (less than 20 or 25 cm) is fixed on to the existing load-bearing walls/roof of a building [43]. The indoor thermal performance achievable in this option is the focus of the current work.

1.1.2. Building insulation usage and thermal comfort in the Indian context

The use of insulation in buildings, though simple to implement, is not widely prevalent in India. There are, however, studies revealing the energy savings potential of using insulation in buildings in India. Natural materials such as bagasse, leaves, etc. [44], wooden boards, [45] and commercial insulation materials such as Extruded Polystyrene (EPS) [46] have been studied for Indian climates. In a review, Gupta et al. [47] noted the suitability of straw as a construction material for buildings in India. The potential for energy and cost savings on implementing straw insulation retrofitting for conditioned spaces in Indian climatic zones was evaluated in a recent work [48] by the current authors. The decision to use any material including straw in the building envelope is intrinsically linked to its thermal performance and the highly subjective and localized thermal comfort preferences of occupants of a building for a particular climate. In a recent review by Sansaniwal et al. [4], the existing thermal comfort standards incorporating the principles of adaptability to varying degrees were briefly described followed by details of thermal comfort studies considering Indian climatic zones. The authors raise an important issue of the lack of an India-specific thermal comfort standard. There has been attempts by Indian researchers to prescribe a standard applicable for India; the Tropical Summer Index (TSI) [49] and Indian Model for Adaptive Comfort (IMAC) [50] being two of the prominent attempts. However, as pointed out by the authors of the review, these are applicable to only certain climate conditions or building types, respectively. Rigid and ill-suited international standards applied to buildings in India lead to excessive energy consumption in the form of air-conditioning load. This is evident from a helpful summary of the ranges of thermal comfort reported in previous literature for the different climatic zones of India included at the end of the review. The climate of India is classified under five zones: warm and humid, composite, cold, hot and dry, and moderate/temperate as per the Energy Conservation Building Code (ECBC) of India [51]. In order to make a more reasonable and practical assessment of the thermal performance of straw insulation, appropriate thermal comfort results and conclusions drawn in literature specific to Indian climates are used throughout the results and discussion section in the current work.

1.1.3. Transient simulation of unconditioned/ventilated spaces

There is a plethora of literature associated with the heat, air, and moisture transfer in buildings with researchers adopting different methods such as whole-building energy simulation software, Computational Fluid Dynamics (CFD) simulation software and more recently, coupled CFD–building simulation software [52]. With high-performance computing resources becoming more affordable, there is more inclination towards full CFD simulation of buildings which remains the best approach to accurately resolve transient conjugate heat transfer and indoor air flow dynamics [53]. Therefore, this brief review covers only recent studies that use CFD tools for analysing indoor airflow and thermal performance of ventilated or unconditioned spaces, some of which are used as references for choosing appropriate simulation parameters. Transient simulation of hygrothermal performance of buildings was carried out by Mirsadeghi [54]. The author had used experimental results available in previous literature to validate the simulations employing standard k–ω model along with low-Re correction and Boussinesq approximation. The thermal comfort in a room ventilated with an impinging jet was examined under different cooling and heating load conditions by Chen et al. [55]. The authors created a model of an office space with external (window, floor) and internal (occupants, computer, and lighting) heat loads. Yang et al. [56] performed transient simulation of buoyancy-driven natural ventilation in a room with heat source considering variations in the temperature difference between the indoor and outdoor space as well as the area, position, and shape of the vent. While the shape and horizontal position of the vent did not have significant effect, thermal comfort was found to decrease with increase in vent area. The effect of simulation parameters such as turbulence model, mesh size, and discretization scheme in predicting the thermal stratification in a heated indoor space was analysed by Gilani et al. [57]. Among five turbulence models analysed, the standard and SST k–ω models were found to reproduce the thermal plume phenomenon successfully. Also, for the structured mesh generated for the 3-D test room, the resolution did not appear to have any significant influence on the indoor air temperature. Piña-Ortiz et al. [58] tested the different turbulent models by comparing the indoor air temperature results from experiments on a ventilated space with and without heat source. The results indicated that the standard k–ω model was the most accurate for the case of heat source turned off while the low Reynolds stress omega model was the most accurate with heat source turned on. Overall, on average, all the turbulence models predicted the indoor air temperature with an error of less than 5%.

Naturally ventilated buildings demand a dedicated study because of the complexities of transient conjugate heat transfer and indoor air flow dynamics. Such studies incorporating insulation-based passive technique are limited in literature [59][60]. Considering the huge generation and wastage of straw residue in India, and with the vast number of existing buildings being naturally ventilated and new buildings being constructed in the country, it is essential to analyse the thermal performance of straw insulation in unconditioned spaces also to arrive at a more complete picture of straw insulation effectiveness in Indian climatic zones.

1.2. Objectives of current work

In the current study, a 3-D model of a representative indoor space is proposed and transient thermal analysis is carried out for a reference uninsulated concrete envelope and for the envelope with straw insulation. The thermal performance of the two envelopes are compared in terms of quantitative parameters such as indoor air temperature, decrement factor (DF), and time lag (TL) as well as qualitative discussion on the need for occupant adaptation such as closing or opening of inlet vent. The assessment of straw insulation performance is done for representative summer and winter days of the five different climatic zones of India. Subsequently, recommendations on the use

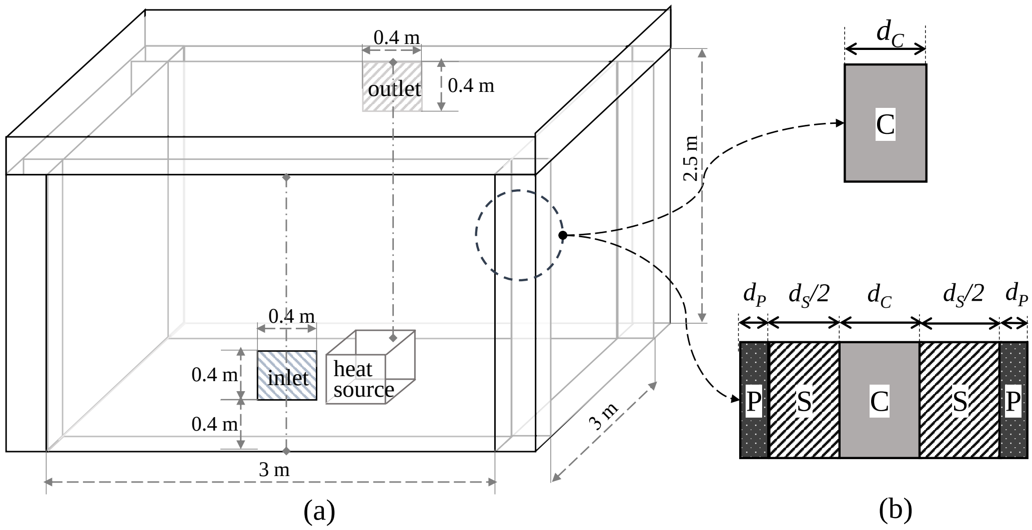

Figure 1: (a) Schematic of the 3-D model of the unconditioned space and (b) the envelope configurations – reference (top) and straw insulation-based (bottom) – consisting of concrete (C), straw (S) and plaster (P) used in the simulation analysis.

of straw insulation are also provided for each zone. Finally, the effects of straw insulation thickness, heat source, inlet air velocity, and position of the straw insulation are also analysed for the extreme warm and cold conditions.

2. Methodology

Transient 3-D conjugate simulation analysis is carried out to assess the thermal performance of the straw-based envelope for an unconditioned space. The model, boundary conditions, and simulation setup are described in this section

2.1. Model of unconditioned space and envelope

A 3-D model with a volume of 22.5 m^3 (3 m × 3 m × 2.5 m) representing an unconditioned space enclosed by envelope (fig. 1a) is proposed for the transient conjugate simulation analysis. Two different configurations of the walls and roof of the envelope are considered as shown in fig. 1b: The first is the reference envelope (denoted by the number '0' in the results) consisting of only load-bearing concrete material (C) of thickness, d_C, equal to 20 cm and the second is the straw insulation-based envelope (denoted by the number '1' in the results). The insulation-based envelope is configured to represent the case of equal thickness ($d_S/2$) of straw (S) insulation retrofitted on to both sides of the concrete material and protected by a plaster (P) layer of thickness, d_P, equal to 2 cm. Such a configuration was found to be the most effective among three possible retrofit configurations (insulation on the outside or on the inside or split equally on either side) [48], and therefore selected for the current analysis. The default thickness of the straw insulation is set as 5 cm on either side of the concrete. The effect of increased thickness of insulation on the thermal performance of the envelope is studied separately in the end. Airflow in the indoor space is promoted by an inlet and an outlet vent. Both the vents have a surface area of 0.16 m^2 (0.4 m $\times$ 0.4 m, vent-to-wall surface area ratio of about 0.0213). The vent-to-wall surface area ratios found in literature were between 0.01 and 0.1 ([61]–[64]). The inlet vent is located on the windward facing wall at a height of 0.4 m from the floor as shown in fig. 1a. The outlet is located at the top middle of the opposing leeward facing wall, as shown in the figure. The windward and leeward facing walls are chosen based on the prevailing wind direction for a particular location and time. The internal heat sources, typically found in residential spaces, is represented by a volume of 0.064 m^3 (0.4 m $\times$ 0.4 m $\times$ 0.4 m) generating a constant heat of 150 W located on the floor in the middle of the indoor space. Typical internal heat loads found in literature had magnitudes of 90 W [65], 100 W [59], or 257 W (95 W occupant, 120 W computer, and 42 W lighting) [55]. So, the internal load of 150 W in the current case is selected in line with the load values used in literature.

2.2. Boundary conditions and material properties

The envelope of the room is specified with the following transient convective boundary condition (eq. (1)) on the outside surface.

$$q_o(t) = h_o(t)(T_{sol}(t) - T_o(t)) \tag{1}$$

where $q_o(t)$ is the outside surface heat flux and $h_o(t)$ is the specified heat transfer coefficient on the outside surfaces of the envelope. T_{sol} (eq. (2)), also specified, is the fictitious sol-air temperature which is a consolidated representation of the outdoor ambient temperature, T_{out}, the total solar radiation, I_t, and the surface characteristics of the envelope (described by h_o, surface emissivity, ϵ_s and surface absorptivity, α_s) as seen in the expression below [66].

$$T_{sol} = T_{out} + \frac{\alpha_s I_t}{h_o} - \frac{\epsilon_s \Delta R}{h_o} \tag{2}$$

Here, $\epsilon_s \Delta R/h_o$ represents the long wave radiation component which, for the current analysis, is assumed to be 0 °C for vertical surfaces (walls) and 4 °C for horizontal surfaces (roof) as per the recommendations in the ASHRAE handbook [66]. The isotropic sky model [67] (eq. (3)) is used to determine the total radiation for each of the walls and the roof.

$$I_t = I_b R_b + I_d \left(\frac{1 + \cos\phi}{2} \right) + I_g \rho_g \left(\frac{1 - \cos\phi}{2} \right) \tag{3}$$

where I_g equals the Global Horizontal Irradiance (GHI), I_d equals the Diffuse Horizontal Irradiance (DHI), and I_b is the product of the Direct Normal Irradiance (DNI) and the cosine of the zenith angle (θ_z). The outside heat transfer coefficient h_o is a combination of convection ($h_{o,conv}$) and radiation ($h_{o,rad}$) components. To estimate the complex convective component [68], the DOE-2 model [69] is selected based on a previous experimental work [18] carried out by the authors. The outside surface boundary condition with a 24-hour time period (single representative day) is repeated until the solution enters a steady periodic state. A location (city or town) in each climate zone of India is chosen (table 2), and the weather and radiation data for the locations are obtained from the online database, National Solar Radiation Database (NSRDB) [70] provided by the National Renewable Energy Laboratory, U.S. The data is obtained for the duration of five years between 2010 and 2014, and the averaged values of outdoor air temperature, wind velocity, and radiation components are used for calculating the transient boundary conditions. This raw data was available for 1 hour time interval and linear interpolation was used to calculate the values for the intermediate time steps. Representative summer and winter days are picked based on the maximum and minimum temperatures, respectively, in the five-year averaged outdoor air temperature data. For all the five zones, the data and the calculated sol-air temperatures under summer and winter conditions are presented in the Appendix section (figures A1 to A10).

The inlet vent is set as a velocity-inlet with time-dependent inlet velocity

Table 2: The climatic zones of India as per ECBC and the selected representative days for summer and winter.

Zone label	Climate condition	Location (Latitude, Longitude)	Summer representative day	Winter representative day
Zone 1 or Z1	Warm and Humid	Chennai (13.08° N, 80.27° E)	May 15	December 15
Zone 2 or Z2	Composite	Jaipur (26.91° N, 75.78° E)	May 15	January 15
Zone 3 or Z3	Cold	Shimla (31.10° N, 77.17° E)	May 15	January 15
Zone 4 or Z4	Hot and Dry	Ahmedabad (23.02° N, 72.57° E)	May 15	January 15
Zone 5 or Z5	Moderate/Temperate	Bengaluru (12.97° N, 77.59° E)	April 15	December 15

and ambient outdoor air temperature values given as input. The magnitude of the velocity is obtained by applying the $1/7^{\text{th}}$ power law approximation (eq. (4)) [71] of the wind speed V_w.

$$v_{inlet}(t) = V_w(t) \times \left(\frac{z}{Z}\right)^{1/7} \tag{4}$$

where the reference wind speed V_w is measured at a height $Z = 10$ m available in the meteorological data and z is the height of the model room. It is assumed that the wall with the inlet is always facing the predominant windward direction decided by the wind direction data for the specific day. Accordingly, other wall orientations are fixed. To simulate a partially closed opening, the velocity magnitude at the inlet is set to a fraction (one-half or one-quarter) of the original value. Also, to simulate a closed inlet, the velocity is set as zero. The outlet is set with a pressure-outlet boundary condition as it is located in the leeward facing wall. For the five climatic zones considered, the calculated inlet velocity never falls below 1 m/s. The characteristic length for the model room is 1.7 m (height difference between the centres of inlet and outlet). Then, the ratio of Gr/Re^2, with the overall average inlet velocity of 1.73 m/s, reaches values of 0.1 or more only when the temperature difference between the indoor air and the inside surface goes beyond 5 °C. Such large temperature differences occur rarely over a day for naturally ventilated buildings. Predominantly, Gr/Re^2 values are less than 0.05 and so, heat transfer owing to free convection is assumed to be insignificant in the current study.

Table 3: Thickness, thermophysical properties, and surface roughness factor of the materials considered

Material	d **(mm)**	ρ **(kg/m^3)**	c **(J/kgK)**	k **(W/mK)**	R_f [68]	α_s
High density concrete (C) ([66], [72])	200	2243	840	1.731	1.52	0.5
Plaster (P) ([73], [74], [75], [76])	20	1600	900	0.7	1.11	0.5
Straw (S) ([77], [78])	100	100	2800	0.08	2.17	0.8

The thermophysical properties of the envelope materials are listed in table 3. The envelope is made of high-density concrete wall of thickness 200 mm whose properties are obtained from ASHRAE handbook [66]. For the plaster coating, suitable thermophysical property values are taken from literature as presented in table 3. Straw insulation with a density of 100 kg/m^3 is selected for which the correlations for effective thermal conductivity and thermal diffusivity of random oriented straw sample [78] are used to obtain the property values. The roughness factor (R_f) which is a part of the DOE-2 model is set for concrete and plaster surfaces as per literature recommendations [68].

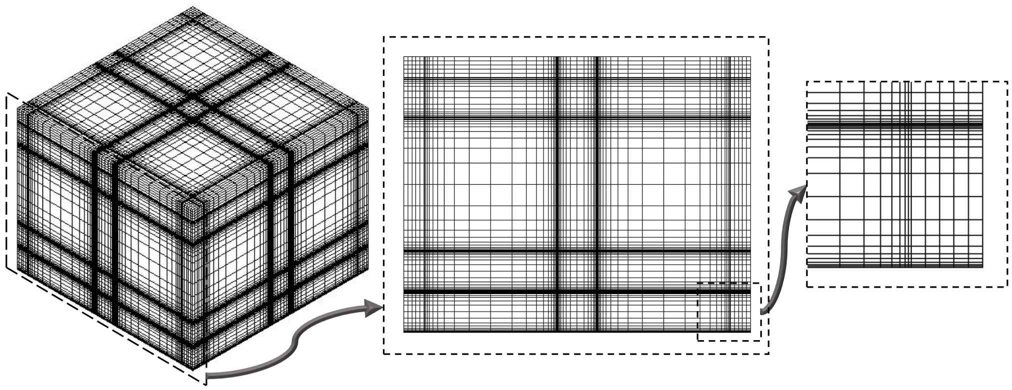

Figure 2: The structured mesh with hexahedral cells generated for the proposed 3-D model room. The inflation layers near the wall boundaries is shown magnified.

Also, the surface is assumed to be opaque and grey with absorptivity α_s values for the materials obtained from literature [72][73][77]. The thermal properties of the straw also varies with moisture content [78]. However, this variation is not considered here because the straw is not directly exposed to the ambient conditions and is protected by plaster layer on both sides. The moisture content in the straw is greatly dependent on the hygroscopic characteristics of the plaster layer [79]. Plaster is a mixture whose hygroscopicity can vary depending on its constituents and their concentration. A plaster layer with low hygroscopicity can be chosen which, in turn, results in negligible influence of the varying moisture of the ambient air on the thermal properties of the straw. Further, the plaster layers enhance the durability of the envelope as they protect the straw from degradation caused by moisture intrusion [10].

2.3. Mesh and simulation setup

The 3-D model is divided into hexahedral cells to create a structured mesh. Figure 2 shows the structured mesh generated for the 3-D model room with the reference envelope which is also used for the grid independence tests. Appropriate inflation layers are generated in the mesh to capture the gradients near the envelope boundaries as well as near the edges of the inlet, the outlet, and the heat source. For the grid independence test, three different structured meshes with varying number of elements and wall boundary first layer thickness are generated as listed in table 4. For the time step independence test, three different time step sizes of 60 s, 120 s, and 300 s are considered and the testing is performed for the chosen mesh following grid independence study.

The transient simulation is carried out using the commercial CFD software, ANSYS Fluent v19.2. Based on the literature review [54][57][58], standard k–ω is selected for turbulence modelling for both the validation simulations as well as the simulations involving the 3-D model room considered in the present study. Pressure–velocity coupling is handled by the SIMPLE

Table 4: Details of the different grids generated to ensure grid independence for the model room.

Mesh	**Number of elements**	**Boundary wall first layer thickness (m)**
Mesh 1 – Coarse	252000	0.00857
Mesh 2 – Normal	416500	0.00476
Mesh 3 – Fine	935750	0.00349

algorithm. The terms in the momentum and energy equations as well as the turbulence parameters are discretized using second order upwind scheme. The transient term is discretized using second-order implicit scheme. Suitable under-relaxation of the velocity results is applied when necessary. The Boussinesq approximation is applied for the air density variation [54][56]. The radiation heat transfer between the inside surfaces is taken care of by the Surface to Surface (S2S) radiation model. The time dependent input variables, namely sol-air temperature and heat transfer coefficient terms present in the envelope outside surface convection boundary condition, and velocity specified at the inlet, which repeat every 24 hours are also specified. The heat source is set as an internal air zone with volumetric heat generation within the indoor air zone.

2.4. Reference cases for validation

Before pursuing the simulations on the current 3-D model room, the setup and procedure along with the chosen grid size and turbulence model need to be validated [80]. For this purpose, two references from literature dealing with different conditions of indoor air simulation are used here. The first is the work by Mirsadeghi [54] in which the author compared the results of transient thermal analysis of an enclosed space using three different methods: only CFD simulation, only Building Energy Simulation (BES) software (ESP-r), and coupled CFD-BES simulation. The geometry of the model is shown in fig. 3a. The cube-shaped enclosed space consists of an envelope of concrete of 8 cm thickness. A step change from 30 °C to 50 °C was given at the northern wall and the resultant transient indoor air temperature profile and the inside surface temperature profile of the north wall are used for the validation. The

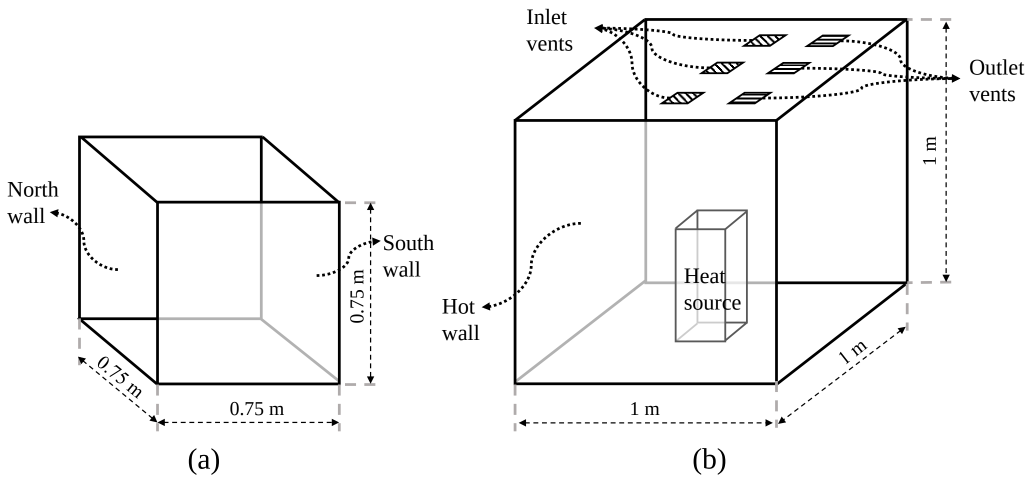

Figure 3: The models used in the references selected for validation: (a) transient simulation of an enclosed space [54] and (b) steady-state simulation and experiment comparative study of a ventilated space [58].

material properties, mesh, and simulation parameters were the same as those used in the reference.

The second reference is a comparative study between experiment and steady-state simulation carried out by Piña-Ortiz et al. [58] with the objective of testing the accuracy of different turbulence models for a ventilated space consisting of a heat source. The scaled ventilated room used for the analysis is shown in fig. 3b. Similar to the proposed model in the current study, the ventilated room has provision for air entry and exit through vents. The authors of the reference work had employed multiple inlet and outlet vents on the roof of the room as opposed to the single inlet and outlet vent on the vertical walls of the current model. For the validation, the near wall temperature profile on the inside surface of the hot wall and the corresponding average heat transfer coefficient value with the heat source turned on are considered.

2.5. Criteria for thermal performance assessment

The effectiveness of straw insulation when compared to the uninsulated envelope for the unconditioned/ventilated indoor space is assessed based on the following criteria:

1. Indoor air temperature extremes and its fluctuation over 24 hours.

2. Decrement factor (DF) and time lag (TL).

3. Need for and extent of occupants' adaptation to improve indoor thermal comfort.

4. Indoor air velocities.

While (1), (2), and (4) comprise of purely quantitative results, the criterion (3) includes a range of quantitative as well as qualitative aspects as listed below:

a) Opening or closing of inlet: can be always open (OPN) or temporarily closed during the day (DAYCLS) or night (NIGHTCLS) or always closed (CLS).

b) Active means of local air circulation (for example, fans): decided based on velocity field in the indoor air space.

c) Active local heating (for example, radiators/fireplace): specified as additional internal heat generation in W on top of the default heat source of 150 W.

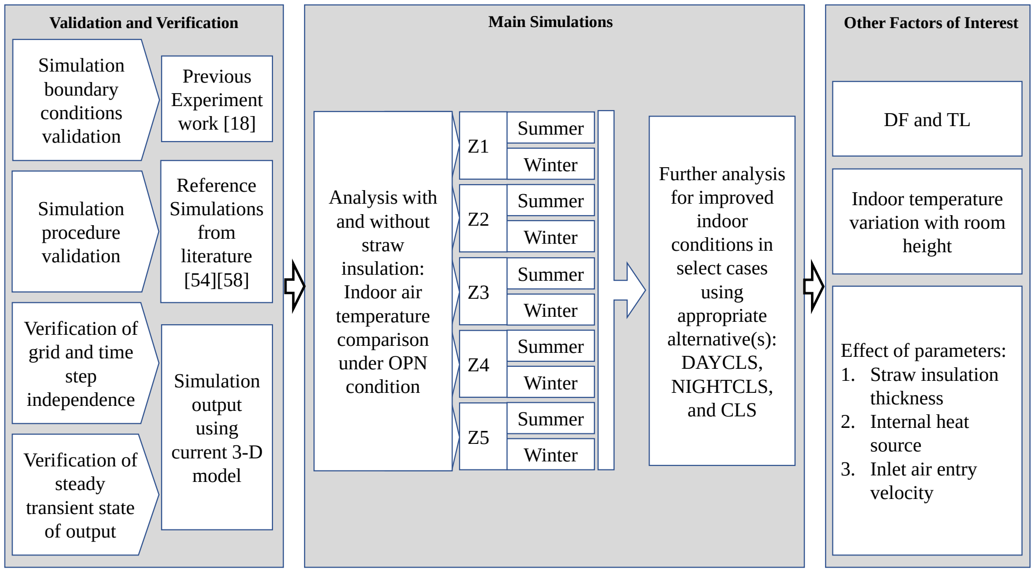

Figure 4: Flowchart depicting the methodology adopted and the various results discussed in the current study.

These aspects vary with zone and prevailing season (summer or winter) depending on requirement. The results and discussion for each zone combines the quantitative and qualitative criteria leading to recommendations for the effective use of straw insulation in the building envelope. The temperature and heat flux results from the simulation are extracted after ensuring a steady transient state is reached. The methodology adopted and the various simulation cases along with the type of the results discussed are shown in a flow chart (fig. 4).

3. Results and discussion

3.1. Results of verification of simulation setup and output

The results of the various aspects of validation, namely validation of the boundary conditions, validation of the simulation procedure, grid and time step independence tests, and verification of attainment of steady-transient state, are presented in this section.

3.1.1. Validation of the boundary conditions

The use of sol-air temperature and its calculation using an appropriate model were validated through experiments conducted on a straw-based outdoor test room. In a previous work by the authors [18], four commonly used models (McAdams, BLAST, MoWiTT, and DOE-2) were compared for estimating the outside surface heat transfer coefficient ($h_{o,conv}$) and subsequently h_o and T_{sol} against the experimental data collected from the test room. The models consider a number of factors influencing the sol-air temperature including wind direction, roughness of the building surface, terrain roughness, and height of the building. The DOE-2 model was found to be giving the results closest to the experimental data. In addition to that, in the work involving the evaluation of energy and cost savings on using the straw insulation in the envelope of a conditioned space [48], the results between the 1-D and 3-D simulations were compared for the experiment duration to reiterate the adequacy of the 1-D model for the analyses carried out on a conditioned space. The DOE-2 model was used in the comparison study as well as later in the transient simulations [48]. Therefore, the DOE-2 model is used in the present study as well.

3.1.2. Validation of the simulation procedure

The results of the validation with the reference works are shown in fig. 5. Both the simulated average indoor air temperature T_{in} (fig. 5a) and the simulated average inside surface temperature of the north wall $T_{N,i}$ (fig. 5b), which is subjected to the step rise in temperature, match well with the reference results. The temperature gradient near the hot wall obtained from the experiment and simulation (using k–ω model) of the reference and the same obtained for the current simulation are compared (fig. 5c). At the surface, the deviation in the temperature value is about 0.4% when compared with that from the experiment. Considering the uncertainty in the temperature measurement being ±0.2% as mentioned in the reference, this is a reasonably good agreement. Further, the average surface convection heat transfer coefficient for the same wall in the current is calculated to be 3.56 W/m^{2}K. The same reported in the reference were 3.6 W/m^{2}K from the simulation (deviation of about 1.1%) and 3.8 W/m^{2}K (deviation of 6.3%) from the experiment. Small variations in the property values of air and grid size is likely to be the cause of the slight deviation observed between the reference and current simulation results.

3.1.3. Grid and time independence results

Before carrying out the main simulations, the proposed 3-D model is subjected to mesh and time step independence tests. The conditions of zone 4 (Ahmedabad – hot and dry) in summer are considered for these tests and the results are presented in fig. 6. The average room air temperature and the inside surface temperatures for the west (windward facing) wall and the roof are compared. With variation in both the mesh (coarse, normal, and

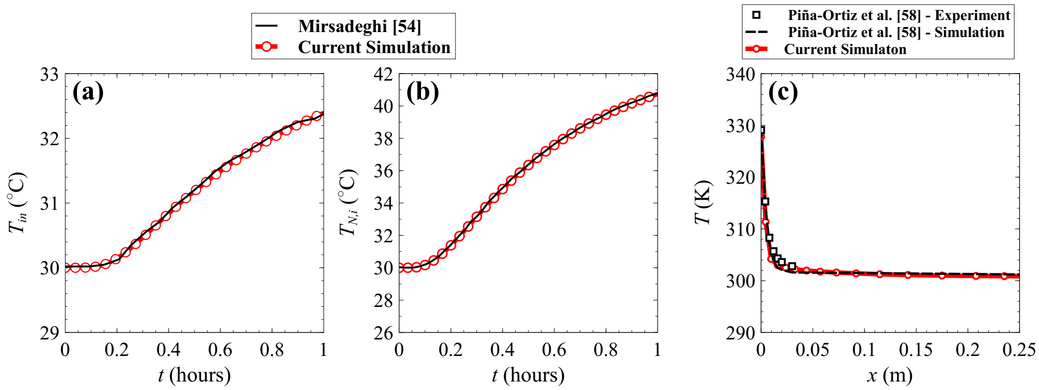

Figure 5: Comparison of the results between the reference and current simulation: (a) average indoor air temperature [54] (b) average inside surface temperature of the north wall [54], and (c) inside surface temperature variation near the hot wall [58].

fine) and time step size (60 s, 120 s, and 300 s), no significant difference in the temperature results are observed. Based on these results, the normal mesh (mesh 2) with a time step size of 300 s are selected for the subsequent simulations.

3.1.4. Steady transient state validity results

It is ensured that the simulation attains a steady transient state before using the 1-day results for further analysis. This is evident in the temperature and heat flux results shown in fig. 7 in which the complete simulation output is shown. Again, the conditions of zone 4 under summer is used for this purpose. For the case of the reference envelope, the simulation is carried out for eight cycles of repeating boundary condition and for the envelope with the straw insulation, the simulation is done for ten cycles. The same number of cycles is employed for the corresponding envelope cases in the subsequent simulations.

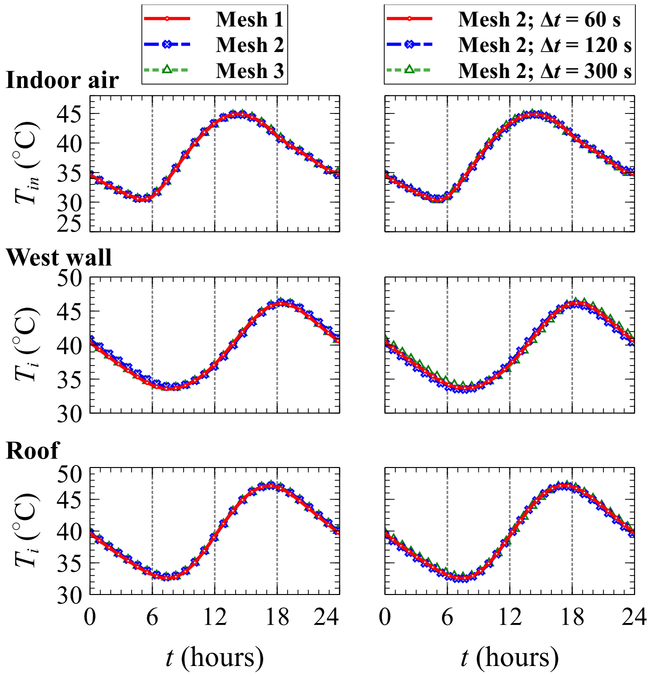

Figure 6: Comparison of indoor air and the surface temperatures of west wall and roof for different grid resolutions and time step sizes.

3.2. Comparison of indoor air temperatures without and with straw insulation

Following the successful validation, the transient simulations for the cases without and with straw insulation in the envelope are taken up next for the different climatic zones of India in summer and winter seasons. Appropriate ventilation modifications are introduced, if necessary, for each condition.

3.2.1. Zone 1: Chennai (warm and humid)

During summer in Chennai, the outdoor air temperature in Celsius consistently reaches mid-30s and occasionally touches 40 °C too. As the city is located near the coastline, there is a high level of humidity in the evening. The results of the comparison of indoor air temperature without and with insulation for this condition are shown in fig. 8. With the inlet vent always

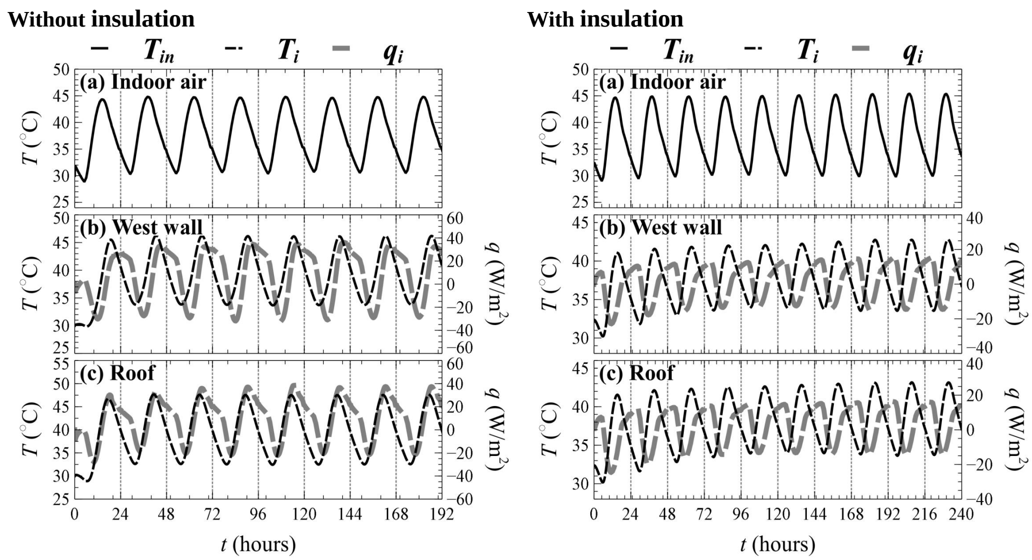

Figure 7: The results of the (a) indoor air temperatures and the inside surface temperatures along with the inside surface heat fluxes for the (b) west wall and (c) roof considering the reference envelope (left) and the envelope with insulation (right) shown for the entire simulation period.

open (OPN), it is observed that the inclusion of straw insulation causes only a slight decrease in the peak indoor air temperature. Further, it is evident that closing the inlet, either temporarily (DAYCLS – closed for 8 hours during the day between 0800 hours to 1600 hours) or always (CLS), is not beneficial in improving the indoor thermal comfort. For the uninsulated reference envelope, temporarily closing the inlet results in a delayed shoot up of the indoor air temperature to nearly 37 °C. With insulation, however, this temperature increase reaches up to a maximum of around 34 °C only. With the inlet always closed, though the indoor air temperature reaches a high value of 37 °C on adding the straw insulation, the fluctuation in the temperature is nearly eliminated. With no insulation, a fluctuation of 5.5 °C exists in the temperature value. This tendency of the insulation to mitigate fluctua-

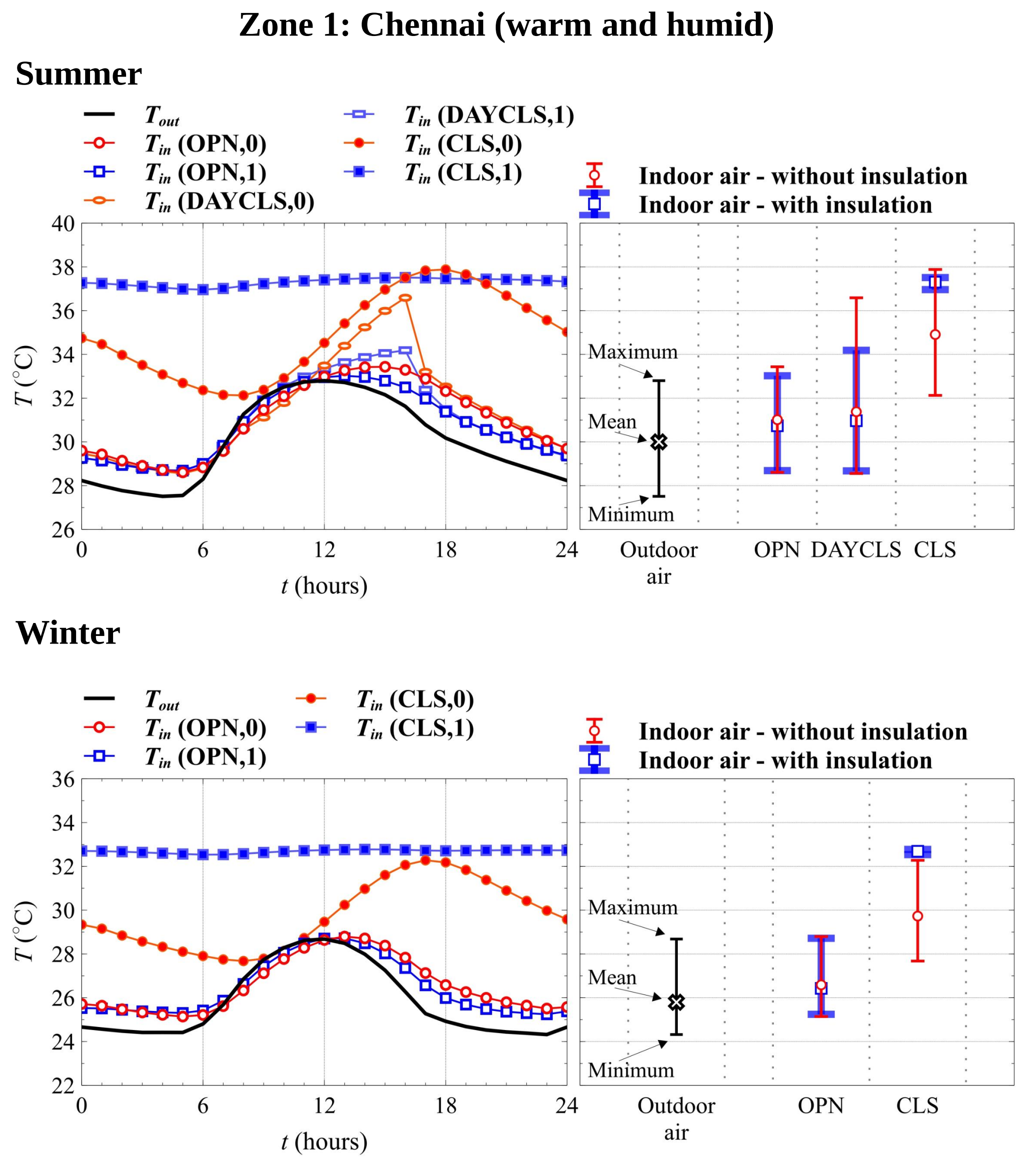

Figure 8: Results for zone 1 (Chennai): Indoor air temperatures for different ventilation conditions compared against the outdoor air temperatures with the corresponding mean and extreme temperature values.

tions in the temperature can be useful during the months between July and September, when the incident radiation is not as high as during the peak summer months between March and May.

Under winter conditions in zone 1, the indoor conditions are relatively comfortable irrespective of the use of insulation as seen from fig. 8. However, during the months of October and November, Chennai receives much of its rainfall which is accompanied by high levels of humidity. Therefore, the inlet may be closed through the day to prevent entry of the moisture-laden air. In such a scenario, without insulation, the indoor temperature remains within a thermally comfortable range but exhibits diurnal fluctuation of about 4 °C. With the straw insulation, this fluctuation is eliminated but a higher temperature of about 33 °C is maintained owing to the heat generated from the internal sources effectively prevented from transferring outside through the envelope.

Overall, in the review by Sansaniwal et al. [4], the comfort temperature range for zone 1, on average, is between 23 °C and 31 °C considering different locations experiencing warm and humid conditions. A field survey conducted in Chennai [81] for apartment buildings estimated an acceptable temperature range of 27 °C to 32 °C with occupant adaptation and proper cross-ventilation. In summer, higher levels of discomfort is reported in the evening hours [82] due to increasing relative humidity. It is found from the simulation results that peak indoor air temperature can be 3 °C to 4 °C lower with straw insulation if the entry of humid air is prevented by temporarily closing the means of air inlet.

The velocity magnitude path lines obtained for the midplane perpendicu-

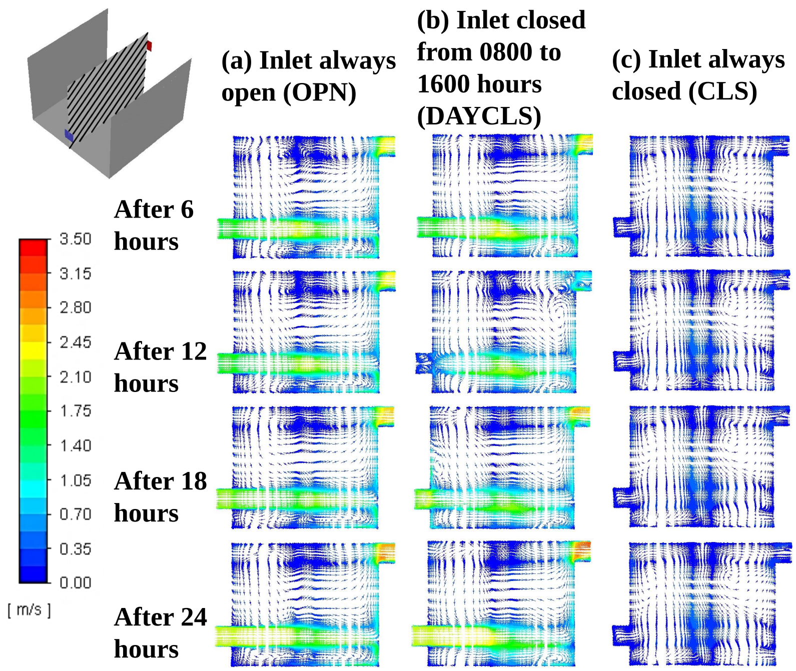

Figure 9: Velocity magnitude path lines at the mid-plane perpendicular to the vents (shown top left) for the different ventilation conditions over six hour intervals for the case of envelope with straw insulation in zone 1, summer.

lar to the vents in the air zone is presented in fig. 9 for the insulated envelope case considering different ventilation conditions. The inlet facilitates air circulation with magnitudes around 2 m/s up to a height of 1.25 m, especially near the heat source. Interestingly, even when the inlet is closed temporarily, air movement of similar velocities are persisting in the room, as seen from the path lines plot after 12 hours in fig. 9b. With inlet always closed, the indoor air velocities drop below 0.5 m/s making active air circulation necessary in this scenario to improve thermal comfort.

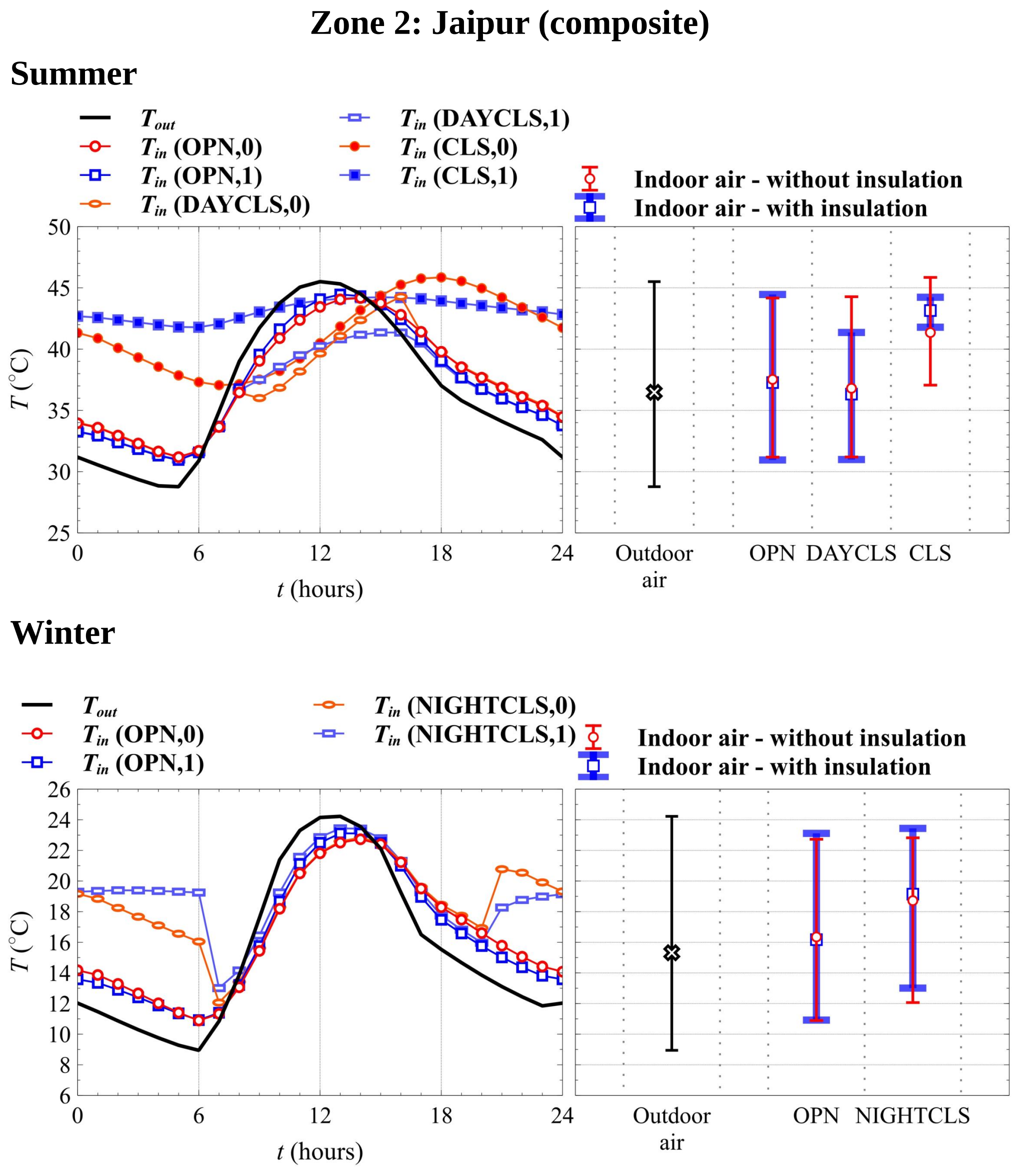

Figure 10: Results for zone 2 (Jaipur): Indoor air temperatures for different ventilation conditions compared against the outdoor air temperatures with the corresponding mean and extreme temperature values.

3.2.2. Zone 2: Jaipur (composite)

The main characteristic of composite climate zone is the extreme seasonal variation. The summers are hot like in zone 4 and winters are cold as in zone 3. Extensive variation in relative humidity is also observed. In summer conditions of zone 2 (fig. 10), the inclusion of straw insulation does not have any effect on the indoor air temperature with the inlet always open with maximum temperature as high as 44 °C. However, on closing the inlet during the day as it was done for summer of zone 1, the peak temperature was reduced to about 41 °C for the insulated envelope. It is also worth noting that unlike zone 1, closing the inlet always does not cause the indoor air temperature to exceed the outdoor air temperature at any time.

Under winter conditions, zone 2 experiences outdoor temperatures as low as 9 °C during late evening/early morning hours. In an effort to prevent the cold air entry, the inlet is closed between 2000 hours and 0600 hours of the next day (NIGHTCLS) and the simulation is carried out. In the 10 hours of closed inlet, it is clear from fig. 10 that the straw insulated envelope is more effective in maintaining a uniform comfortable temperature of 19 °C. Opening or closing the inlet causes a sudden decrease or increase in the indoor air temperature, respectively. Closing the inlet for a longer duration in the morning (say, up to 1000 hours) can negate the temperature swing.

Occupants of naturally ventilated buildings living in composite climate were generally found to have wider perception of comfort temperature [4]. Kumar et al. [83] estimated a maximum comfort temperature of 34.5 °C for naturally ventilated buildings with indoor air speeds of 1 m/s. Additional air circulation is obtainable by means of table or ceiling fan. During the peak of summer as seen in the representative day selected in the current simulation, the indoor conditions are predominantly uncomfortable even with the broader comfort range. Therefore, additional means of lowering the temperature, either passive or active, to complement the envelope insulation are necessary for such occasions.

3.2.3. Zone 3: Shimla (cold)

The main characteristics of cold climate of zone 3 is relatively comfortable conditions in summer but less than desirable outdoor ambient temperature in the winter. Under summer conditions, the option of inlet kept closed during the day rather than the night is analysed. This is because the existing literature show occupants prefer temperatures between 20 °C to 25 °C [4] as they are accustomed to the cold climate. At night, the outdoor air temperature reaches only 1 °C to 2 °C lower than the minimum comfort temperature. Therefore, the occupant is more likely to close the inlet during the day when the outdoor temperature exceeds the maximum comfort temperature by nearly 7 °C. Though the straw insulation does not show much benefit with the inlet vent always open, a drop in temperature fluctuation by 3 °C is achieved when the inlet is closed during the day (DAYCLS) as seen in fig. 11.

The addition of straw insulation in the building envelope is most effective in the winter condition of the cold climate zone as observed in fig. 11. As for the inlet condition, it is evident that keeping the inlet closed is the most suitable option to trap the heat generated from sources within the indoor space. This is achieved with the indoor temperature maintained at around 14 °C with insulation while without the insulation, the mean temperature is

Zone 3: Shimla (cold)

Summer

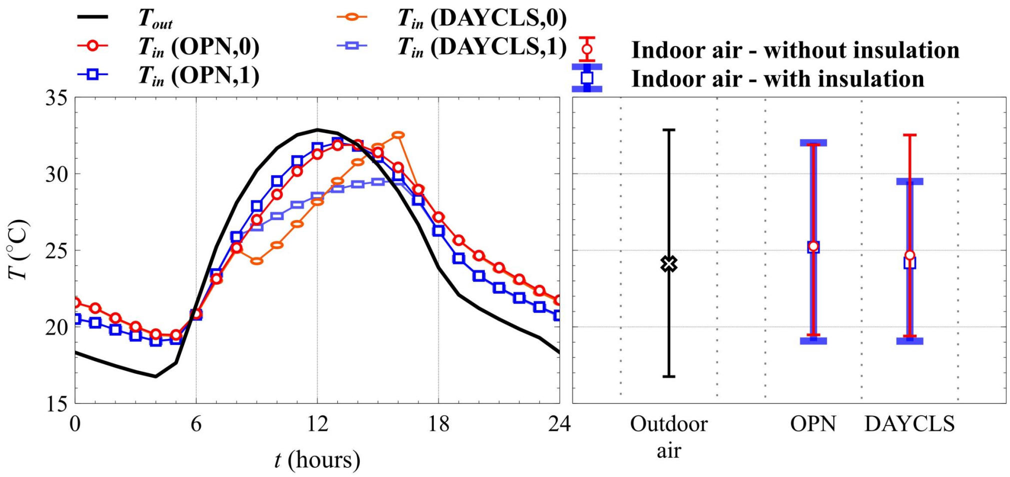

Winter

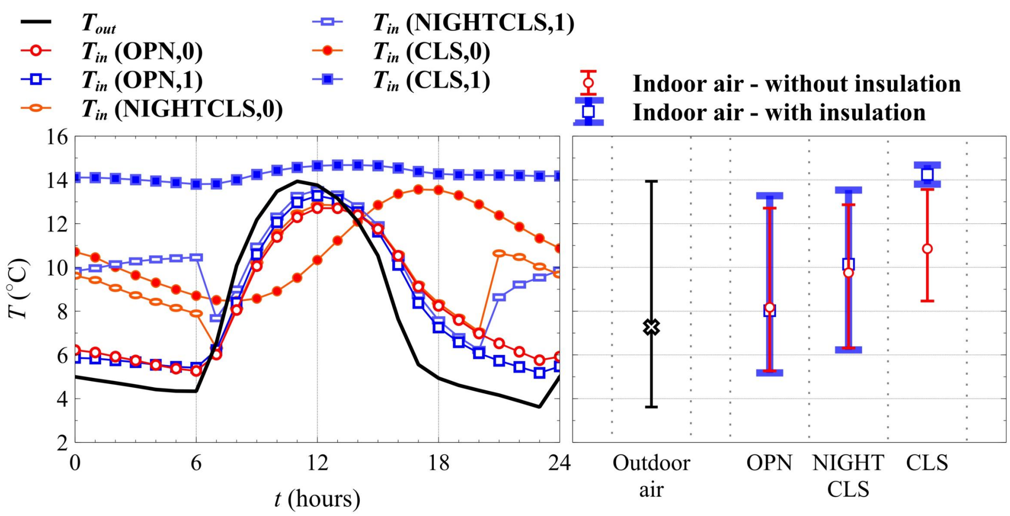

Figure 11: Results for zone 3 (Shimla): Indoor air temperatures for different ventilation conditions compared against the outdoor air temperatures with the corresponding mean and extreme temperature values.

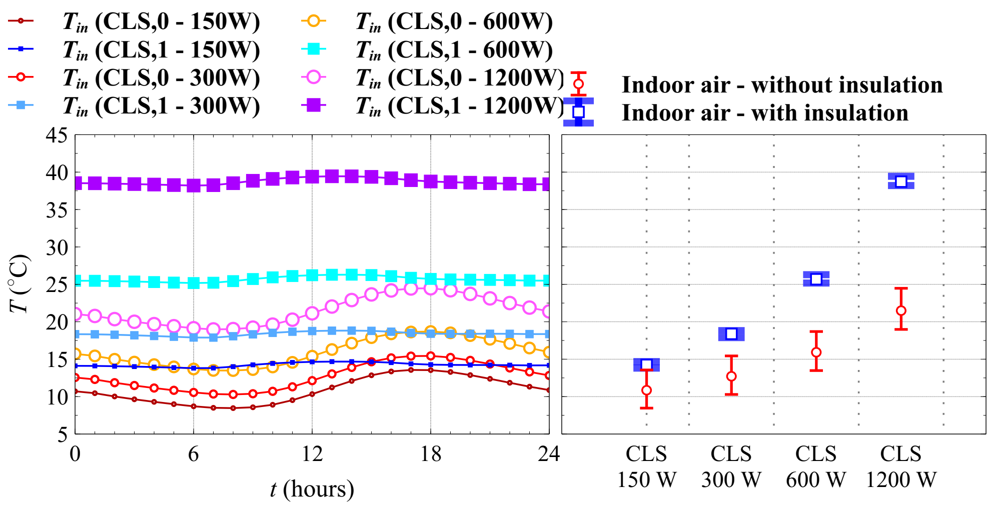

Figure 12: Indoor air temperatures for different internal heat sources and the corresponding mean and extreme temperature values for winter conditions of zone 3.

about 11 °C with fluctuation of about 6 °C. To reach thermally comfortable condition, additional active heating is necessary. In the current analysis, this additional heating is represented by increasing the magnitude of total internal heat generation to 300 W, 600 W, and 1200 W. The corresponding indoor air temperatures achieved are shown in fig. 12 for the reference as well as the envelope with insulation cases. Temperatures between 18 °C and 26 °C can be achieved with the total internal heat source value ranging between 300 and 600 W when the straw insulation is present. The same level of indoor temperature is possible only with a heat source of 1200 W or more when no insulation is employed. For all heat source values, the fluctuation is only about 1 °C to 2 °C with insulation as opposed to 5 °C without insulation.

Zone 4: Ahmedabad (hot and dry)

Summer

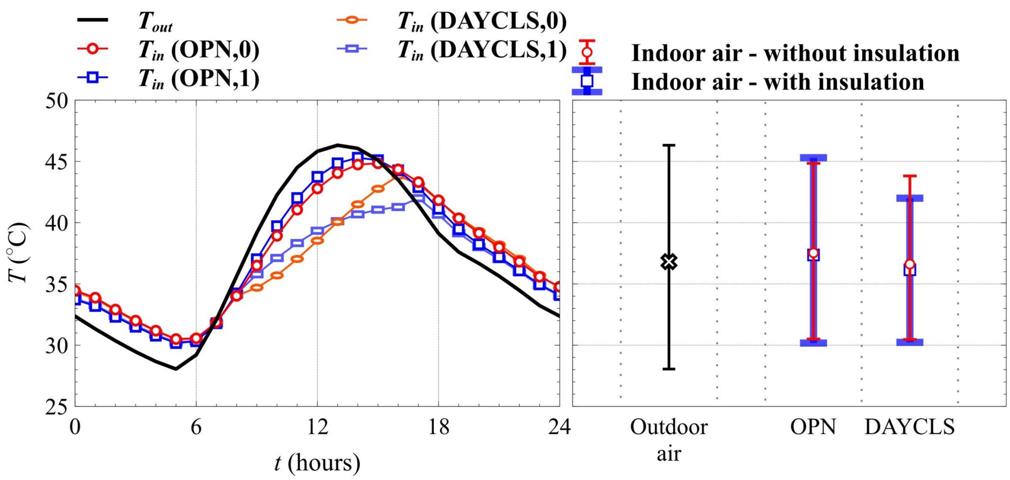

Winter

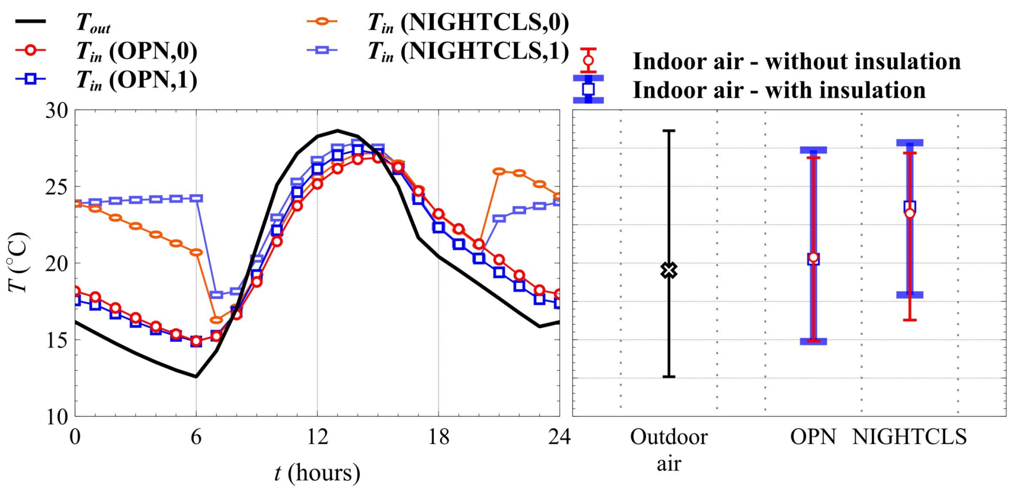

Figure 13: Results for zone 4 (Ahmedabad): Indoor air temperatures for different ventilation conditions compared against the outdoor air temperatures with the corresponding mean and extreme temperature values.

3.2.4. Zone 4: Ahmedabad (hot and dry)

The hot and dry conditions of zone 4 feature high outdoor ambient temperatures at times touching 45 °C. The outcome of the simulation is similar to that of the summer conditions of the composite (zone 2) climate. Straw insulation was found to be beneficial for the case of the inlet temporarily closed during the day (DAYCLS) as seen in fig. 13. The peak indoor temperature was reduced by about 2.5 °C compared to that case of the reference envelope. As the occupants are used to a higher temperature range in the summer season, it is preferable to avoid low temperatures in the winter conditions. Therefore, the option of the inlet closed temporarily during the night (between 2000 hours to 0600 hours) is analysed for the winter condition as shown in fig. 13. As in the case of the winter conditions of zone 2, the duration of the closed inlet may be extended to avoid abrupt changes in the indoor temperature.

The velocity magnitude path lines (fig. 14) show air movement within the indoor space. Even with the inlet closed, air circulation is observed in the plots after 24 hours and after 6 hours facilitated by the internal heat source and the outlet. This air circulation can be enhanced with the help of table or ceiling fans to improve the indoor thermal comfort. For the locations directly in line with the inlet, air velocities of around 1 m/s is noticeable throughout the day. Udaykumar et al. [84] reported a comfort temperature range between 25 °C and 31 °C for summer and between 21.5 °C to 27 °C for winter in the hot and dry climate of Ahmedabad. Also, the acceptance of higher temperatures increased when air speeds of 1 m/s was available. While straw insulation improves the indoor comfort conditions

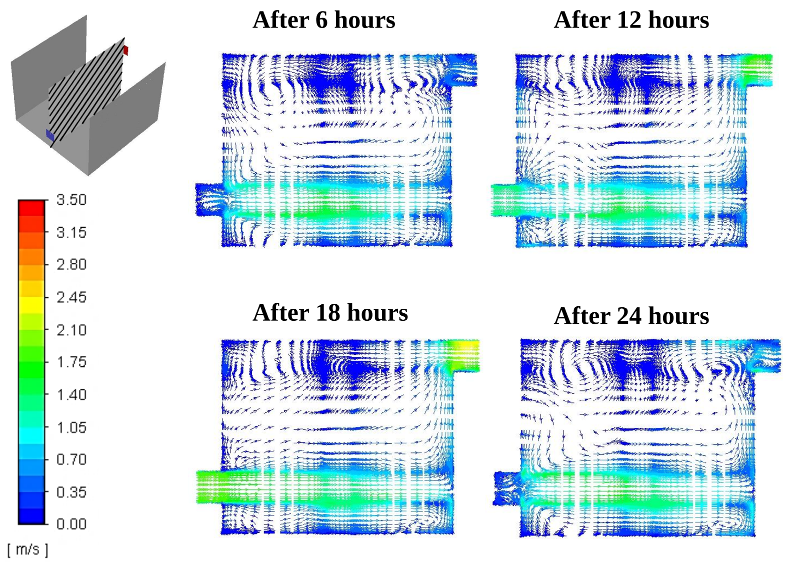

Figure 14: Velocity magnitude path lines at the mid-plane perpendicular to the vents (shown top left) for NIGHTCLS condition over six hour intervals for the case of envelope with straw insulation in zone 4, winter.

during winter and to some degree in the milder summer months, additional measures complementing the building insulation are necessary during peak summer.

3.2.5. Zone 5: Bengaluru (temperate/moderate)

The prevailing outdoor conditions in the temperate zone rarely reaches a point of severity. Therefore, naturally ventilated buildings can provide comfortable indoor conditions throughout the year with the least occupant adaptation requirements. As there is no major seasonable shift, the simulation results of summer and winter conditions are presented together in fig. 15. As the air entering the building does not have a significant cooling or heating effect, it is desirable to keep the inlet always open from a thermal

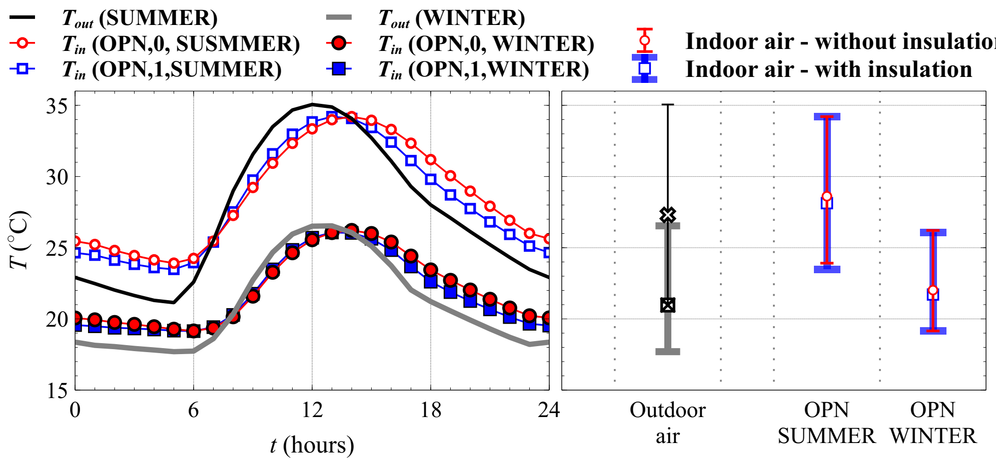

Figure 15: Results for zone 5 (Bengaluru): Indoor air temperatures compared against the outdoor air temperatures with the corresponding mean and extreme temperature values.

comfort point of view. Unsurprisingly, the use of insulation is least effective for buildings in this zone. The indoor air remains within a range of 19 °C and 34 °C over the summer and winter representative days.

3.3. Decrement factor and time lag

The standard definition of decrement factor is the ratio of the difference between the maximum and minimum temperatures at the inside surface to the same at the outside surface and is represented as DF_{surf} in eq. (5).

$$DF_{surf} = \frac{T_{i,max} - T_{i,min}}{T_{o,max} - T_{o,min}} \quad (5)$$

Generally, the lower the decrement factor, the better the effectiveness of insulation of the building envelope. The results of the DF_{surf} obtained on averaging the decrement factors obtained for the various walls and roof are presented in fig. 16. The effectiveness of the straw insulation in inhibiting

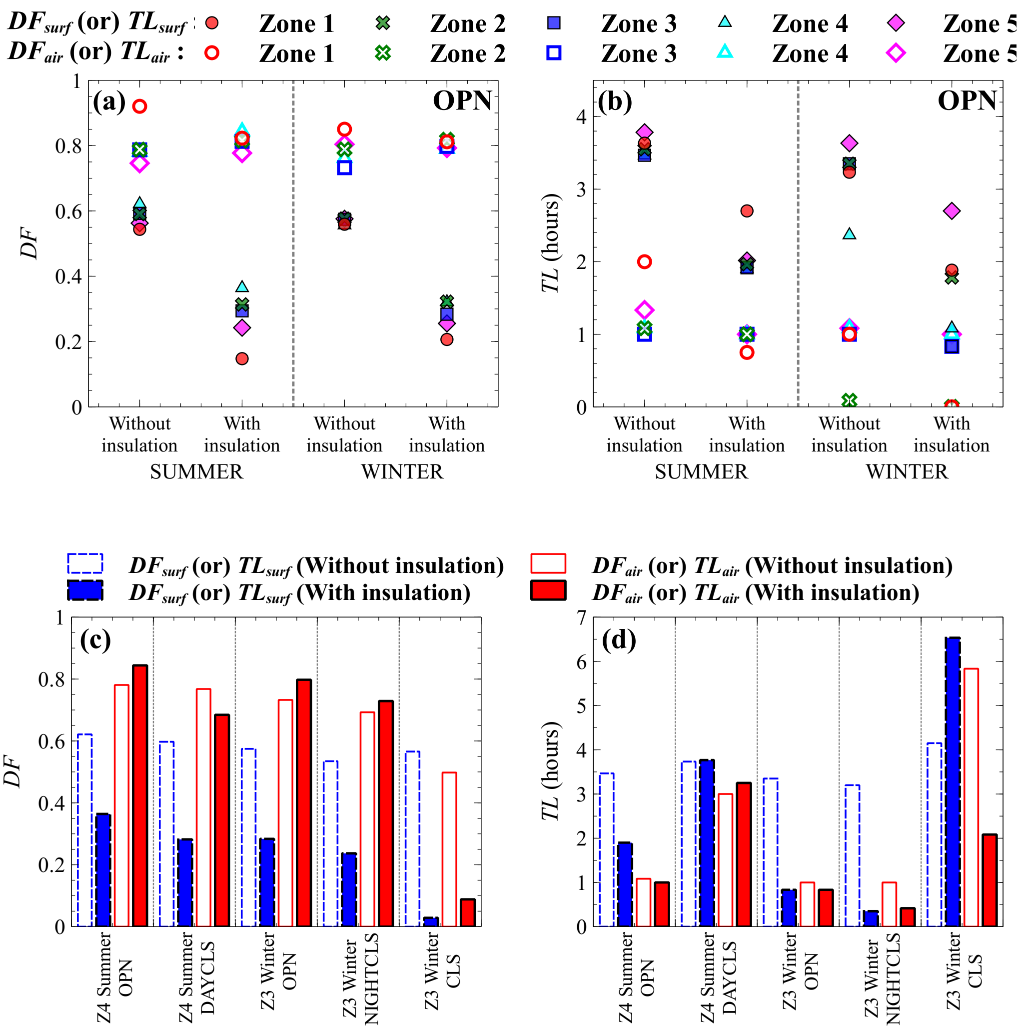

Figure 16: The DF_{surf} and DF_{air} values (a) across different zones under OPN condition and (c) for different ventilation conditions of zones 3 and 4. The TL_{surf} and TL_{air} values (b) across different zones under OPN condition and (d) for different ventilation conditions of zones 3 and 4.

the heat transfer through the envelope is clear from the reduction of DF_{surf} to about half of the same obtained for the envelope without insulation across all the zones for both summer and winter as seen in fig. 16a. Also, for the reference envelope, the ventilation condition (OPN, CLS, DAYCLS, NIGHT-

CLS) does not have any significant effect on the DF_{surf} values as observed in fig. 16c. Though the DF_{surf} results imply effective indoor thermal management on adding straw insulation, the results from the previous section show that this benefit is not reflected in the indoor air temperatures. Therefore, for ventilated spaces, a more appropriate decrement factor would be in terms of the indoor and the outdoor air temperatures indicated as DF_{air} in eq. (6).

$$DF_{air} = \frac{T_{in,max} - T_{in,min}}{T_{out,max} - T_{out,min}} \tag{6}$$

The DF_{air} results in fig. 16a reflect the temperature results obtained in the previous section. The influence of air entering through the inlet vent on the indoor conditions is clearly captured in the CLS case of zone 3 seen in fig. 16c in which a drastic reduction in DF_{air} is obtained compared to the same for the ventilated (OPN, DAYCLS, and NIGHTCLS) cases.

Time lag is typically expressed as the time interval in hours between the occurrence of the maximum temperature on the inside and outside surfaces and is represented as TL_{surf} in eq. (7).

$$TL_{surf} = t_{T_{i,max}} - t_{T_{o,max}} \tag{7}$$

Typically, a time lag of 8 to 10 hours ensures shifting of peak load to late evening hours enabling better management of the HVAC energy demand in air-conditioned buildings. For naturally ventilated or mixed-mode ventilated buildings, it is difficult to interpret the time lag values in such a straight forward manner and requires discussion of the same in the context of prevailing conditions. So, similar to DF_{air}, TL_{air} is defined (eq. (8)) with respect to air temperatures.

$$TL_{air} = t_{T_{in,max}} - t_{T_{out,max}} \tag{8}$$

The results of TL_{surf} and TL_{air} are presented in fig. 16b and fig. 16d. TL_{surf} values are in the range of 3 to 4 hours for the reference envelope on average across the different zones while addition of straw insulation causes the TL_{surf} to reduce to about 2 hours. Although a greater shift in the peak surface temperature is seen beneficial to manage cooling load in fully air-conditioned buildings, this can be detrimental to indoor thermal comfort in naturally ventilated buildings especially in humid conditions. High humidity as a result of moist air entering through the inlet vent combined with shifted high indoor temperature will create a stiflingly uncomfortable condition in the evening. Therefore, a lower value of time lag is acceptable for unconditioned spaces when the prevailing conditions are warm and humid as in zone 1. On analysing the modified time lag values (TL_{air}) for both without and with insulation in fig. 16b and fig. 16d, it is evident that the air flow through the inlet vent is the driving factor behind the time of occurrence of peak indoor temperature irrespective of the presence or absence of insulation. The time lag values increase by about 2 hours when the inlet vent is closed during day as seen in summer conditions of zone 4.

3.4. Indoor air temperature variation with height

The indoor air temperature variation with the height of the model room is plotted in fig. 17 for the extreme conditions of summer in zone 4 and winter in zone 3. A maximum temperature variation of 1 °C along the

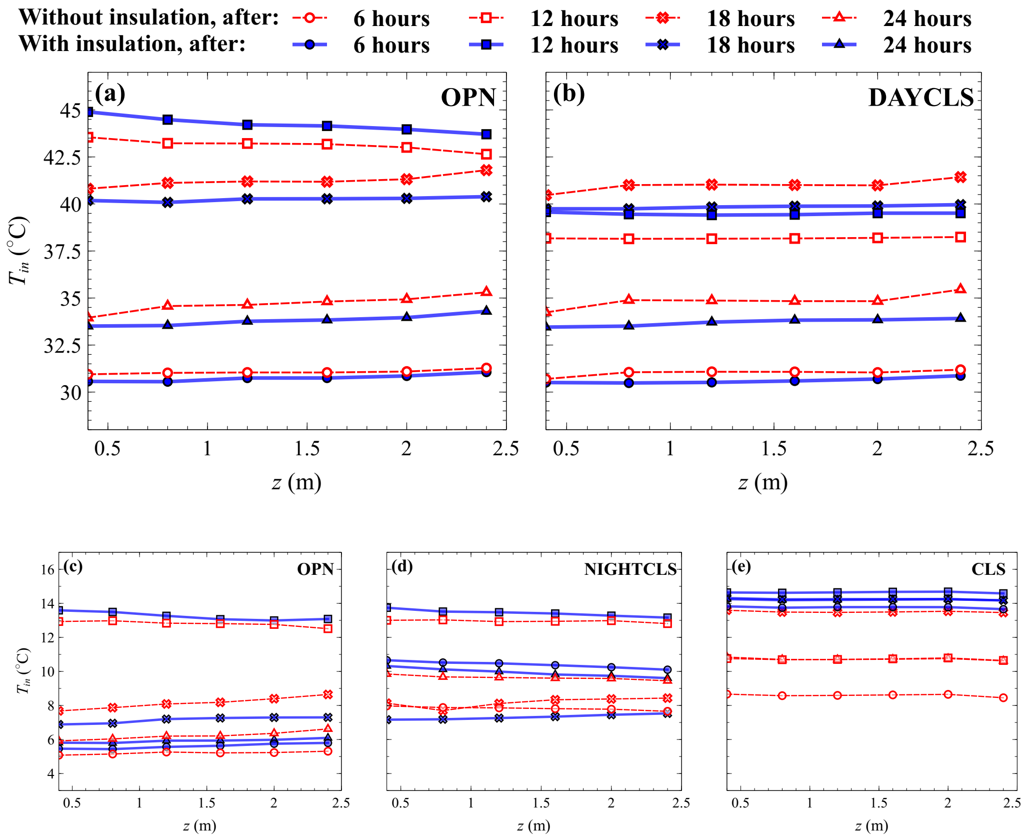

Figure 17: Indoor air temperature variation with height after every six hours for the representative days of (a) OPN and (b) DAYCLS conditions of summer in zone 4 and (c) OPN, (d) NIGHTCLS, and (e) CLS conditions of winter in zone 3.

height of the room is observed for zone 4. As expected, warm air entry through the inlet results in indoor air having a slightly higher temperature near the bottom close to the inlet after 12 hours while the air temperature changes to being slightly higher near the top after 18 hours as seen in fig. 17a. The addition of insulation tends to reduce the temperature variation and is approximately 0.5 °C, except at 12 hours. With the inlet vent closed during day (DAYCLS), a more uniform temperature across the different heights of the room is obtained. This is evident by comparing the temperature plots after 12 hours in fig. 17a and fig. 17b. The results for zone 3 confirm the dominating effect of air flow on the uniformity of air temperature with respect to height.

3.5. Effect of different parameters

This section presents the effects of different parameters such as straw insulation thickness, heat source, air entry velocity, and location of straw insulation on the transient thermal performance of the naturally ventilated room.

3.5.1. Straw insulation thickness

The effect of higher insulation thickness of 20 cm (10 cm on either side of the concrete) is studied for the two extreme conditions: summer of zone 4 (Ahmedabad) and winter of zone 3 (Shimla). The indoor air temperature results for the simulations are presented in fig. 18a and fig. 18b and compared with the same for the insulation thickness of 10 cm. It is evident that for naturally ventilated buildings with vents always open, increase in the thickness of insulation has only marginal effect on the indoor air temperature for both the zones.

To understand the reasons for the relative ineffectiveness of insulation in naturally ventilated buildings, the rate of heat transfer into and out of the test room is analysed for the summer conditions of zone 4. The total heat Q added to (in positive value) and removed from (in negative value) the indoor air at every hour of the day is shown in figures 19a, 19b, and 19c. Here, Q_{source} is the 150 W heat added by the heat source in the room throughout the day and Q_{env} is the rate of total heat transfer evaluated at the inside surface of the different envelope orientations and is a result of the transient heat conducted through the envelope, which is equal to the convection heat transfer between the envelope inside surface and the room air and the net radiation exchange between the inside surfaces. Q_{vent} is the net heat transported through the vents. The values of Q_{env} and Q_{vent} plotted are obtained from the hourly solution reports from the simulations. Integrating the three components of heat transfer over 24 hours gives the total energy flow in Whr for each. For example, in the 10 cm insulated case, integrating over Q_{env}, Q_{vent}, and Q_{source} amount to 2617 Whr, -6095 Whr, and 3600 Whr, respectively. The addition or removal of heat through the envelope is affirmed by the difference between the average inside surface temperature ($\overline{T_i}$) and the indoor air temperature (T_{in}). Similarly, the difference between the air temperature at the inlet vent (T_{inlet}) and the air temperature at the outlet vent (T_{outlet}) confirms the direction of the net heat transported through

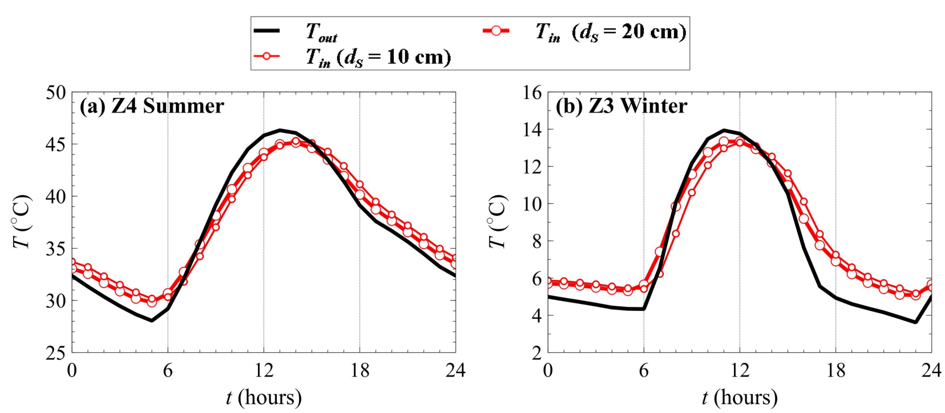

Figure 18: The effect of increasing the straw insulation thickness from 10 cm to 20 cm on the indoor air temperature for (a) summer of zone 4 (Ahmedabad) and (b) winter of zone 3 (Shimla).

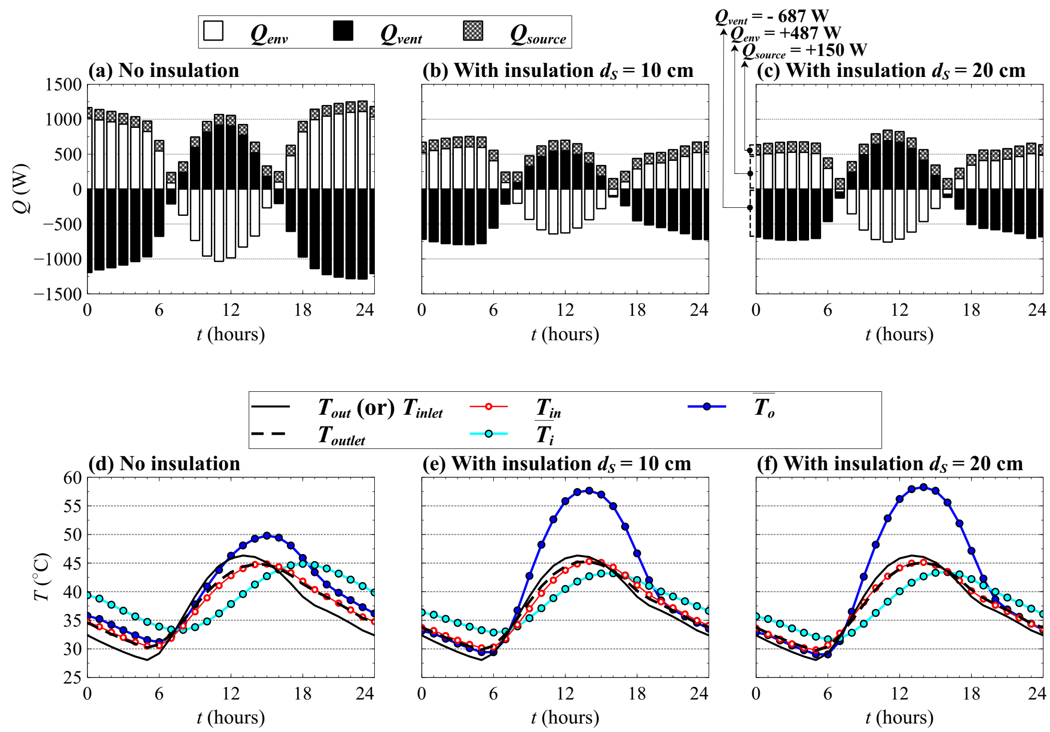

Figure 19: Heat (Q) added to/removed from the indoor air through different means compared ((a), (b), and (c)) and the various temperature results ((d), (e), and (f)) for the three insulation conditions in summer of zone 4.

the vents. These temperatures are plotted in figures 19d, 19e, and 19f.

The minimum average indoor temperature possible is the minimum outer ambient temperature. With the inlet vent open, the maximum average indoor temperature largely depends on the maximum outer ambient temperature and is also influenced by the heat source and the heat transfer between the envelope and the room air, depending on the thermal inertia and insulation effect of the envelope. However, with the inlet vent closed or partially closed, the effect of envelope and insulation on the indoor temperature will be significant, as discussed in section 3.2. In figures 19a, 19b, and 19c, there are several interesting aspects worth discussing. The first is the time intervals during which each of the heat flow components contributes toward heating of the indoor air. The heat addition through the vents occurs during midday between 0800 hours and 1500 hours while the heat addition through the envelope occurs during the rest of the day. Therefore, any beneficial effect caused by the insulation in the envelope is likely to be noticed only before 0800 hours and after 1500 hours. Consequently, figures 19d and 19e reveal that the indoor air temperature is nearly 4 °C higher than the outdoor air temperature for the envelope without insulation while the indoor air temperature is close to the minimum possible outdoor air temperature when insulation is present. On the other hand, the lack of insulation turns out to be advantageous during the midday hours as more heat is removed through the envelope, which is also evident from the inside surface temperature being lower than the average temperature of the indoor air. It is also noticeable in fig. 19a that a relatively larger amount of heat is added or removed by air flow through vents. Table 5 shows that higher values of the average heat transfer coefficient, h, are obtained when there is no insulation owing to greater temperature difference between the inside surface and the indoor air. The east (leeward) wall inside surface directly faces the air entering through the inlet in the west (windward) wall thereby exhibiting h values nearly 3 to 3.5 times the same for the west.

3.5.2. Heat source

The results of the indoor air temperatures with and without heat source for summer of zone 4 and winter of zone 3 when the straw insulation is included in the envelope are presented in fig. 20a and fig. 20b, respectively. The "no heat source" condition is simulated by setting the internal heat

Table 5: Overall average heat transfer coefficients on the inside surface of the different envelope orientations.

Orientation	***h* (W/m^{2}K)**	
	No insulation	**With insulation**
West (windward)	3.6	3.7
East	12.5	11.2
North	5.2	4.5
South	5.0	4.4
Roof	3.6	3.0

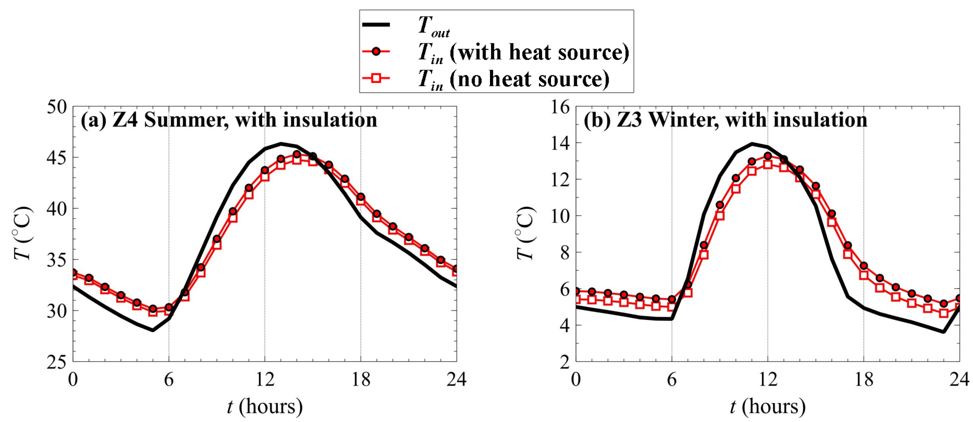

Figure 20: The effect of heat source on the indoor air temperature for summer of zone 4 (Ahmedabad) and (b) winter of zone 3 (Shimla).

generation as 0 W in the simulation setup. In the heat balance analysis carried out for the summer of zone 4 in the previous section, it was found that the hourly Q_{source} values were three to four times lesser than the Q_{env} and Q_{vent} values for most of the day. However, the integral values over 24 hours show that the contribution of Q_{source} is comparable with the contributions of Q_{env} and Q_{vent}. Figure 20a shows that the removal of the heat source causes a maximum decrease of 0.6 °C in the indoor air temperature for the summer conditions of zone 4. For the winter of zone 3, the same level of decrease is observed. While the 0.6 °C drop is exhibited for a short interval

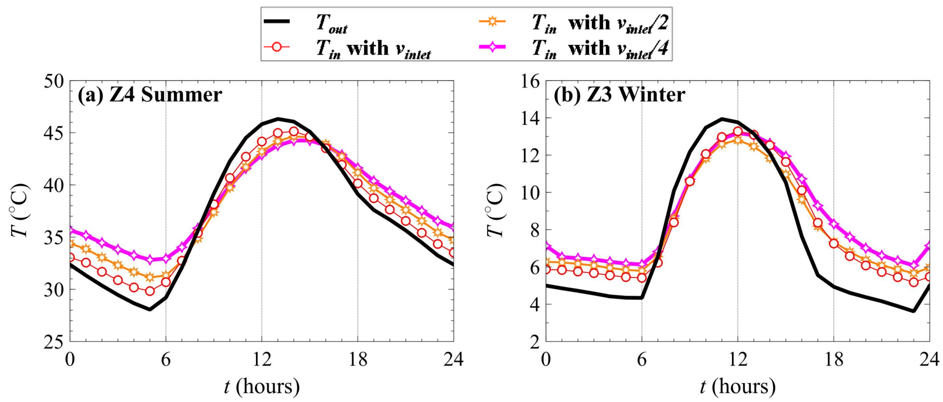

Figure 21: The effect of reducing the air velocity at the inlet to half and quarter the original value on the indoor air temperature for (a) summer of zone 4 (Ahmedabad) and (b) winter of zone 3 (Shimla).

(about 4 to 5 hours) in zone 4, it is prevalent almost throughout the day in zone 3. Although this temperature difference does not seem appreciable, it is still comparable with the effects on the indoor air temperature caused by the addition of insulation and therefore has an effect on the overall thermal performance of the test room.

3.5.3. Air entry velocity

The effect of partially closing the inlet is simulated by reduced values of air velocity applied as boundary conditions at the inlet. The results of the indoor air temperature for the summer of zone 4 and winter of zone 3 when the indoor air velocity is lowered by half ($v_{inlet}/2$) and by one quarter ($v_{inlet}/4$) throughout the day are presented in fig. 21a and fig. 21b, respectively. The reduction of air velocity causes an increase in the indoor air temperature which is detrimental for summer of zone 4 while beneficial for zone 3 winter conditions.

The velocity magnitude depicted in fig. 22 for the summer of zone 4 shows

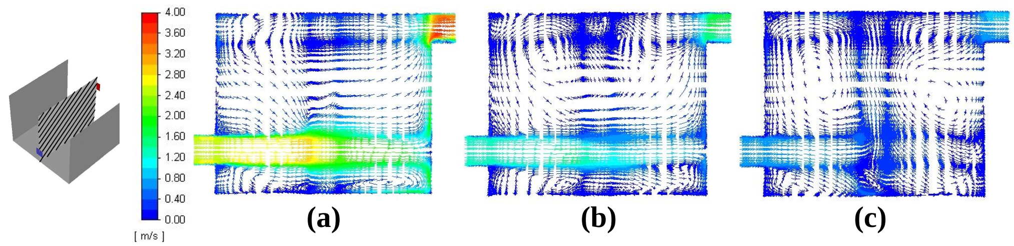

Figure 22: Velocity magnitude path lines at the mid-plane perpendicular to the vents for inlet velocities of (a) v_{inlet} (b) $v_{inlet}/2$ and (c) $v_{inlet}/4$ after 24 hours in the case of envelope with straw insulation for summer conditions of zone 4.

the resultant lower air velocities in the indoor air caused by reducing the inlet velocity by one-half and one-quarter. More air circulation is noticeable for lower inlet velocities and these are centred at a lower height when the inlet velocity is set as one-fourth of the original (fig. 22c) compared to the case of half the original velocity (fig. 22b). In terms of magnitude, apart from the region near the vents, not much difference is observable between the two low velocity cases, as the room cross-sectional area (9 m^2) is much larger than the vent cross-sectional area (0.16 m^2).

3.5.4. Relocation of straw insulation

The choice of selecting the position of straw insulation in the building envelope was based on the thermal analysis carried out for conditioned space [48]. In reality, it is more convenient and easily implementable to retrofit the straw insulation only on the outside surface of the building envelope. With no additional insulation on the inside, shrinking of the indoor floor area is also avoided. Considering these benefits, the effect of positioning the 10 cm thick straw insulation on the outside is studied by comparing the resulting indoor air temperature with the same from the configuration of 5 cm straw placed on either side presented earlier. The comparison performed again for

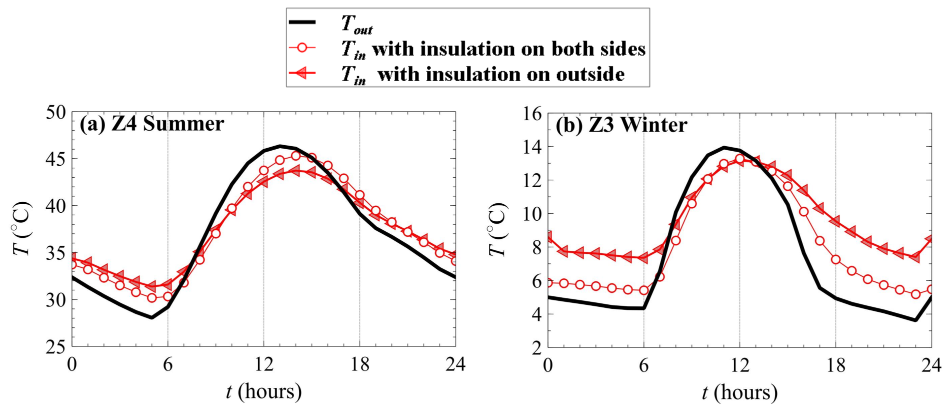

Figure 23: The effect of repositioning the straw insulation of 10 cm thickness to the outside on the indoor air temperature for (a) summer of zone 4 (Ahmedabad) and (b) winter of zone 3 (Shimla).

the two extreme cases of summer in zone 4 and winter in zone 3 are presented in fig. 23a and fig. 23b, respectively.

Interestingly, at first glance, there is an indication that positioning the straw insulation on the outside is more effective in maintaining better indoor thermal conditions than when the straw is equally split on either side of the envelope. There is a contrasting effect observed for the two zones. For the summer of zone 4, repositioning of the straw causes a reduction in the peak temperature by nearly 2 °C, but this reduction does not cause a significant reduction in the mean temperature over 24 hours. In the winter of zone 3, on the other hand, the maximum temperature remains the same while an increase of 1.5 °C is caused by repositioning of the straw to the outside.

Comparing the thermal analysis of ventilated space in the current work and conditioned space from a previous work [48] for the same representative days of Indian climatic zones, it is clear that air flow through the vents has a major impact on the resulting indoor thermal conditions. For a conditioned space (with the indoor temperature maintained constant), the effectiveness of straw insulation in greatly reducing the heating or cooling loads was beyond doubt. This is also reaffirmed in the current work on analysing the results of the case of inlet always closed (CLS) performed for a few conditions which comes closest to resembling a closed space in the conditioned buildings. In the winter conditions of zone 3, from the previous work, it was observed that more energy savings was achievable for the configuration of insulation equally split on either side than the configuration of insulation placed on the outside. However, in terms of indoor air temperature in the current work, placing straw on the outside produced slightly better results. This is an indication that the conclusions drawn on the basis of analysis done on a conditioned space may not strictly apply to an unconditioned space even for a simplistic model with a single inlet and outlet.

4. Conclusions

In the current work, 3-D simulations of unconditioned space with a reference concrete envelope and a plaster protected straw insulation-based envelope were performed considering different ventilation conditions during representative summer and winter days of the various climate zones of India. The major conclusions are:

1. With the inlet vent always open allowing for air entry and consequently better natural ventilation in the indoor space, across the five zones over summer and winter conditions, the ranges of the variations in the mean, maximum, and minimum indoor air temperatures with respect to the outdoor air temperature were +0.7 °C to +1.3 °C, -1.8 °C to +0.6 °C,

and +0.8 °C to +2.8 °C, respectively, when there is no straw insulation in the envelope. Similarly, with the insulation in the envelope, the corresponding ranges of variations were +0.5 °C to +1.1 °C, -1.2 °C to +0.2 °C, and +0.9 °C to +2.3 °C. With the removal of the internal heat source, a maximum decrease in the indoor air temperature of 0.6 °C was obtained which is comparable with the above temperature variations.

2. A small change in the indoor air temperatures with straw insulation when the inlet vent is always open is due to the heat transport through the vent openings having a dominant impact on the indoor temperature under steady transient conditions. Heat balance analysis performed for the summer conditions of zone 4 showed that during the interval between 0800 hours and 1500 hours, air entering through the inlet vent is largely responsible for the heat addition to the indoor air, thus forcing the insulation to play the adverse role of inhibiting heat removal from the indoor air. Though the uninsulated envelope allows more heat to enter the indoor space, it is equally good in removing the heat.

3. Increasing the straw insulation thickness from 10 cm to 20 cm does not have a significant effect on the indoor air temperature for both hot (summer of zone 4) and cold (winter of zone 3) conditions. When the 10 cm insulation is wholly positioned on the outside, contrasting effects on the indoor air temperature were observed for the zones 4 and 3. In the summer conditions of zone 4, there is a reduction in the peak temperature by 2 °C, but no appreciable difference in the mean temperature over 24 hours. In the winter of zone 3, the maximum temperature is

unaffected, while there is a reduction in the mean temperature by 1.5 °C.

4. With the aim of improving indoor thermal conditions for some climate zones, the inlet vent can be closed temporarily or throughout the day. In summer conditions, to prevent warm air entering the indoor space, the inlet vent is closed between 0800 hours to 1600 hours. For the case of the straw-based envelope, the temporary closing of inlet during the day resulted in the reduction in the peak indoor temperature by 3 °C to 4 °C in zones 2, 3, and 4. When there is no insulation present, closing of inlet during the day has little (1 °C to 2 °C reduction in peak indoor air temperature for zone 4) or no (other two zones) benefit.

5. In winter conditions, the aim is to prevent loss of heat generated from internal sources. Therefore, the inlet is closed between 2000 hours to 0600 hours of the next day inhibiting the entry of colder outdoor air. For the winter conditions of zones 2 and 4, the indoor conditions are improved, more so with the insulated envelope, on closing the inlet during the night. It is also clear that the thermal comfort can be further improved if the closing of inlet is extended by two to three hours in the morning in these two zones.

6. There are situations where the inlet may be closed always. For example, in the winter of zone 3, the entry of cold air may not be desirable throughout the day. In this condition, additional active heating is needed to achieve thermal comfort. With the straw insulation, the required heating does not exceed 600 W while without insulation, at

least 1200 W of heating is necessary. There are also other reasons such as walls of adjacent buildings or foliage causing air entry in the inlet to be obstructed or absent. The resulting poor natural ventilation makes it necessary to implement additional means (passive or active) of achieving thermal comfort. In such cases, the straw insulation is effective in minimizing the fluctuations in the indoor air temperature as seen from the simulation results with inlet always closed in various zones.

7. The results of the velocity path lines plotted for the indoor space show air flow with velocities between 1 and 1.5 m/s up to a height of 1.25 m owing to the combination of the wind-driven air entering the inlet and the heat source. For the cases in which the inlet is closed throughout the day, the air velocity drops to less than 0.5 m/s.

8. With respect to the height of the model room, the air temperature remains more or less uniform, varying by a maximum of approximately 1 °C without insulation and 0.5 °C with insulation. When the inlet vent is closed, the variation in the room temperature with height is less than 0.5 °C owing to the diminished influence of the outdoor air.

9. There was a recurring trend of decrement values reduced by about half when straw insulation was included in the envelope when compared with that for the reference envelope. This confirms the capability of the straw materials as an effective means of blocking heat entry through the building envelope. However, a more appropriate representation of indoor conditions is given by modifying the definitions of *DF* and *TL*

in terms of the indoor and outdoor air temperatures, for the ventilated spaces.

In naturally ventilated buildings, the assessment of effectiveness of straw insulation is complicated owing to variations in building design and elevation, site terrain, presence of obstructions to wind-driven air entry, solar shading, prevailing climate, and so on. The current work shows that occupant adaptation strategies can play a key role in ensuring the optimized use of straw insulation in buildings in different climate conditions. Control of air entry to the indoor space is an easily adoptable occupant strategy investigated in this work and with straw insulation-based envelope some of the strategies explored through simulation analyses proved to be beneficial in mitigating the peak indoor temperature. Nonetheless, more research is required, both experimental and theoretical, to investigate the additional complexities, which can lead us to the improved understanding of the thermal comfort in naturally ventilated buildings and the role of cost-effective insulations such as straw in achieving it. The effect of a permeable hygroscopic plaster on the hygrothermal performance of the envelope and more varied user behaviour are two such complexities worth exploring further.

Conflict of interest

None

Acknowledgments

The current work is part of the doctoral research carried out by the first author, Karthik Sabapathy who gratefully acknowledges the scholarship provided by the Ministry of Human Resource Development, Government of India. The authors thank the High Performance Computing Environment (HPCE) team at the P. G. Senapathy Centre for Computing Resources at IIT Madras for making available the resources to perform the numerical simulations in the current work.

References

[1] G. Zia, A. Agrawal, B. Patel, S. Mehrotra, A. Sinha, N. Shetty, S. Sarkar, M. Bhoir, T. Bhowmick, Brick by Brick Moving towards 'Housing for all', Technical Report, RICS and Kinght Frank, 2019.

[2] R. Tongia, S. Gross, Coal in India, Technical Report, 2019. URL: http://hdl.handle.net/11540/9782.

[3] P. Dean, B., Dulac, J., Petrichenko, K., and Graham, Towards a zero-emission, efficient, and resilient buildings and construction sector, 2016. URL: https://www.worldgbc.org/sites/default/files/GABC_Global_Status_Report_V09_november_FINAL.pdf.

[4] S. K. Sansaniwal, J. Mathur, V. Garg, R. Gupta, Review of studies on thermal comfort in Indian residential buildings, Science and Technology for the Built Environment 26 (2020) 727–748. doi:10.1080/23744731.2020.1724734.

[5] A. Mahdavi, S. Kumar, Implications of indoor climate control for comfort, energy and environment, Energy and Buildings 24 (1996) 167–177. doi:10.1016/S0378-7788(96)00975-9.

[6] S. B. Sadineni, S. Madala, R. F. Boehm, Passive building energy savings: A review of building envelope components, Renewable and Sustainable Energy Reviews 15 (2011) 3617–3631. doi:10.1016/j.rser.2011.07.014.

[7] R. Rawal, Y. Shukla, Residential Buildings in India : Energy Use Projections and Savings Potentials, Technical Report, Global Buildings Performance Network (GBPN), 2014.

[8] B. King, Straw bale construction, Building Standards (1998) 18–24.

[9] J. C. McCabe, The Thermal Resistivity of Straw Bales for Construction, Master's thesis, The University of Arizona, 1993.

[10] P. Walker, A. Thomson, D. Maskell, Straw bale construction, Elsevier, 2016. doi:10.1016/B978-0-08-100038-0.00006-8.

[11] C. H. A. Koh, D. Kraniotis, A review of material properties and performance of straw bale as building material, Construction and Building Materials 259 (2020). doi:10.1016/j.conbuildmat.2020.120385.

[12] A. Thomson, P. Walker, Durability characteristics of straw bales in building envelopes, Construction and Building Materials 68 (2014) 135–141. doi:10.1016/j.conbuildmat.2014.06.041.

[13] S. Devi, C. Gupta, S. L. Jat, M. S. Parmar, Crop residue recycling for economic and environmental sustainability: The case of India, Open Agriculture 2 (2017) 486–494. doi:10.1515/opag-2017-0053.

[14] P. Kumar, S. Kumar, L. Joshi, The Extent and Management of Crop Stubble, in: Socioeconomic and Environmental Implications of Agricultural Residue Burning, Springer India, New Delhi, 2015, pp. 13–34.

[15] N. Jain, A. Bhatia, H. Pathak, Emission of air pollutants from crop residue burning in India, Aerosol and Air Quality Research 14 (2014) 422–430. doi:10.4209/aaqr.2013.01.0031.

[16] H. Ribeiro, Sugar cane burning in Brazil: respiratory health effects, Rev. Saude Publica 42 (2008).

[17] X. Yin, M. Lawrence, D. Maskell, Straw bale construction in northern China – Analysis of existing practices and recommendations for future development, Journal of Building Engineering 18 (2018) 408–417. doi:10.1016/j.jobe.2018.04.009.

[18] K. A. Sabapathy, S. Gedupudi, In situ thermal characterization of rice straw envelope of an outdoor test room, Journal of Building Engineering 33 (2020) 101416. doi:10.1016/j.jobe.2020.101416.

[19] B. Marques, A. Tadeu, J. Almeida, J. António, J. de Brito, Characterisation of sustainable building walls made from rice straw bales, Journal of Building Engineering 28 (2020) 101041. doi:10.1016/j.jobe.2019.101041.

[20] R. Gallegos-Ortega, T. Magaña-Guzmán, J. A. Reyes-López, M. S. Romero-Hernández, Thermal behavior of a straw bale building from data obtained in situ. A case in Northwestern México, Building and Environment 124 (2017) 336–341. doi:10.1016/j.buildenv.2017.08.015.

[21] O. Douzane, G. Promis, J. M. Roucoult, A. D. Tran Le, T. Langlet, Hygrothermal performance of a straw bale building: In situ and laboratory investigations, Journal of Building Engineering 8 (2016) 91–98. doi:10.1016/j.jobe.2016.10.002.

[22] K.-I. I. Lee, D. Yeom, Experimental research on the indoor environment control of natural insulation materials: Carbonized rice hull and straw bales, Indoor and Built Environment 24 (2015) 729–739. doi:10.1177/1420326X14534866.

[23] G. Verbeeck, J. Ponet, Straw bale houses in a moderate climate adaptable to meet future energy performance requirements?, Proceedings - 28th International PLEA Conference on Sustainable Architecture + Urban Design: Opportunities, Limits and Needs - Towards an Environmentally Responsible Architecture, PLEA 2012 (2012).

[24] K. Wall, P. Walker, C. Gross, C. White, T. Mander, Development and testing of a prototype straw bale house, Proceedings of the Institution of Civil Engineers - Construction Materials 165 (2012) 377–384. doi:10.1680/coma.11.00003.

[25] G. Garas, M. Allam, Thermal performance of plastered rice straw bales and walls: a case study, International Journal of Sustainable Development and Planning 6 (2011) 226–237. doi:10.2495/SDP-V6-N2-226-237.

[26] T. Ashour, H. Georg, W. Wu, Performance of straw bale wall: A case

of study, Energy and Buildings 43 (2011) 1960–1967. doi:10.1016/j.enbuild.2011.04.001.

[27] K. Holzhueter, K. Itonaga, The hygrothermal environment and potential for mold growth within a straw bale wall, Journal of Asian Architecture and Building Engineering 9 (2010) 495–499. doi:10.3130/jaabe.9.495.

[28] C. Whitman, D. Fernandez, The viability of improving energy efficiency and hygrothermal comfort of rural social housing in central chile using straw bale construction (2010).

[29] S. T. Elias-Ozkan, F. Summers, N. Surmeli, S. Yannas, A comparative study of the thermal performance of building materials, PLEA 2006 - 23rd International Conference on Passive and Low Energy Architecture, Conference Proceedings (2006) 6–8.

[30] A. Mesa, A. Arenghi, Hygrothermal behaviour of straw bale walls: experimental tests and numerical analyses, Sustainable Buildings 4 (2019) 3. doi:10.1051/sbuild/2019003.

[31] X. Yin, M. Lawrence, D. Maskell, W.-S. S. Chang, Construction and monitoring of experimental straw bale building in northeast China, Construction and Building Materials 183 (2018) 46–57. doi:10.1016/j.conbuildmat.2018.05.283.

[32] J. Robinson, H. K. Aoun, M. Davison, Determining Moisture Levels in Straw Bale Construction, Procedia Engineering 171 (2017) 1526–1534. doi:10.1016/j.proeng.2017.01.390.

[33] F. D'alessandro, F. Bianchi, G. Baldinelli, A. Rotili, S. Schiavoni, Straw Bale Constructions: Laboratory, in Field and Numerical Assessment of Energy and Environmental Performance, Journal of Building Engineering 11 (2017) 56–68. doi:10.1016/j.jobe.2017.03.012.

[34] F. Liu, Y. Liu, S. Wang, J. Fan, Thermal performance study on the energy saving and environment protection sandwich block wall with straw blocks, in: 2nd International Conference on Waste Engineering and Management, 2010.

[35] S. Hou, F. Liu, S. Wang, H. Bian, Coupled heat and moisture transfer in hollow concrete block wall filled with compressed straw bricks, Energy and Buildings 135 (2017) 74–84. doi:10.1016/j.enbuild.2016.11.026.

[36] R. Ahmadi, B. Souri, M. Ebrahimi, Evaluation of wheat straw to insulate fired clay hollow bricks as a construction material, Journal of Cleaner Production 254 (2020) 120043. doi:10.1016/j.jclepro.2020.120043.

[37] A. D. González, Energy and carbon embodied in straw and clay wall blocks produced locally in the Andean Patagonia, Energy and Buildings 70 (2014) 15–22. doi:10.1016/j.enbuild.2013.11.003.

[38] M. Labat, C. Magniont, N. Oudhof, J.-E. E. Aubert, From the experimental characterization of the hygrothermal properties of straw-clay mixtures to the numerical assessment of their buffering potential, Building and Environment 97 (2016) 69–81. doi:10.1016/j.buildenv.2015.12.004.

[39] J. Zhang, J. Wang, S. Guo, B. Wei, X. He, J. Sun, S. Shu, Study on heat transfer characteristics of straw block wall in solar greenhouse, Energy and Buildings 139 (2017) 91–100. doi:10.1016/j.enbuild.2016.12.061.

[40] B. Belhadj, M. Bederina, Z. Makhloufi, A. Goullieux, M. Quéneudec, Study of the thermal performances of an exterior wall of barley straw sand concrete in an arid environment, Energy and Buildings 87 (2015) 166–175. doi:10.1016/j.enbuild.2014.11.034.

[41] T. Ashour, A. Korjenic, S. Korjenic, W. Wu, Thermal conductivity of unfired earth bricks reinforced by agricultural wastes with cement and gypsum, Energy and Buildings 104 (2015) 139–146. doi:10.1016/j.enbuild.2015.07.016.

[42] K. Wei, C. Lv, M. Chen, X. Zhou, Z. Dai, D. Shen, Development and performance evaluation of a new thermal insulation material from rice straw using high frequency hot-pressing, Energy and Buildings 87 (2015) 116–122. doi:10.1016/j.enbuild.2014.11.026.

[43] A. R. Bertorello, A technological analysis applied to existing building insulated with straw, Key Engineering Materials 600 (2014) 719–726. doi:10.4028/www.scientific.net/KEM.600.719.

[44] H. K. Singh, R. Prakash, K. K. Shukla, Economic insulation thickness of external walls in hot and composite regions of India, in: Global conference on Renewable energy GCRE2016, 2016, p. 6.

[45] K. Kulkarni, P. Sahoo, M. Mishra, Optimization of cooling load for a lecture theatre in a composite climate in India, Energy Build. 43 (2011) 1573–1579. doi:10.1016/j.enbuild.2011.02.015.

[46] T. Ramesh, R. Prakash, K. Shukla, Life cycle approach in evaluating energy performance of residential buildings in indian context, Energy Build. 54 (2012) 259–265. doi:10.1016/j.enbuild.2012.07.016.

[47] M. S. Gupta, U. K. Roy, M. Roy, R. K. Gupta, Monika S. Uttam, Roy, Expediting faster housing supply in India using straw bale as prefab building material, 2019. doi:10.1016/b978-0-12-803581-8.11664-9.

[48] K. A. Sabapathy, S. Gedupudi, On the influence of concrete-straw-plaster envelope thermal mass on the cooling and heating loads for different climatic zones of India, Journal of Cleaner Production (2020) 123117. doi:10.1016/j.jclepro.2020.123117.

[49] M. R. Sharma, S. Ali, Tropical summer index-a study of thermal comfort of Indian subjects, Building and Environment 21 (1986) 11–24. doi:10.1016/0360-1323(86)90004-1.

[50] S. Manu, Y. Shukla, R. Rawal, L. E. Thomas, R. de Dear, Field studies of thermal comfort across multiple climate zones for the subcontinent: India Model for Adaptive Comfort (IMAC), Building and Environment 98 (2016) 55–70. doi:10.1016/j.buildenv.2015.12.019.

[51] Bureau of Energy Efficiency, Energy Conservation Building Code for Residential Buildings (Part I: Building Envelope Design), Technical Report, 2005.

[52] H. Wang, Z. J. Zhai, Advances in building simulation and computational techniques: A review between 1987 and 2014, Energy and Buildings 128 (2016) 319–335. doi:10.1016/j.enbuild.2016.06.080.

[53] Q. Chen, Ventilation performance prediction for buildings: A method overview and recent applications, Building and Environment 44 (2009) 848–858. doi:10.1016/j.buildenv.2008.05.025.

[54] M. Mirsadeghi, Co-simulation of building energy simulation and computational fluid dynamics for whole-building heat, air and moisture engineering, 2011. doi:10.6100/IR694412.

[55] H. J. Chen, B. Moshfegh, M. Cehlin, Investigation on the flow and thermal behavior of impinging jet ventilation systems in an office with different heat loads, Building and Environment 59 (2013) 127–144. doi:10.1016/j.buildenv.2012.08.014.

[56] X. Yang, K. Zhong, H. Zhu, Y. Kang, Experimental investigation on transient natural ventilation driven by thermal buoyancy, Building and Environment 77 (2014) 29–39. doi:10.1016/j.buildenv.2014.03.013.

[57] S. Gilani, H. Montazeri, B. Blocken, CFD simulation of stratified indoor environment in displacement ventilation: Validation and sensitivity analysis, Building and Environment 95 (2016) 299–313. doi:10.1016/j.buildenv.2015.09.010.

[58] A. Piña-Ortiz, J. F. Hinojosa, J. P. Xamán, J. M. Navarro, Test of turbulence models for heat transfer within a ventilated cavity

with and without an internal heat source, International Communications in Heat and Mass Transfer 94 (2018) 106–114. doi:10.1016/j.icheatmasstransfer.2018.03.021.

[59] J. Zhou, G. Zhang, Y. Lin, Y. Li, Coupling of thermal mass and natural ventilation in buildings, Energy and Buildings 40 (2008) 979–986. doi:10.1016/j.enbuild.2007.08.001.

[60] A. Gagliano, F. Nocera, F. Patania, A. Moschella, M. Detommaso, G. Evola, Synergic effects of thermal mass and natural ventilation on the thermal behaviour of traditional massive buildings, International Journal of Sustainable Energy 35 (2016) 411–428. doi:10.1080/14786451.2014.910517.

[61] J. Tanny, V. Haslavsky, M. Teitel, Airflow and heat flux through the vertical opening of buoyancy-induced naturally ventilated enclosures, Energy and Buildings 40 (2008) 637–646. doi:10.1016/j.enbuild.2007.04.020.

[62] J. I. Perén, T. van Hooff, B. C. Leite, B. Blocken, CFD analysis of cross-ventilation of a generic isolated building with asymmetric opening positions: Impact of roof angle and opening location, Building and Environment 85 (2015) 263–276. doi:10.1016/j.buildenv.2014.12.007.

[63] M. Jin, W. Liu, Q. Chen, Simulating buoyancy-driven airflow in buildings by coarse-grid fast fluid dynamics, Building and Environment 85 (2015) 144–152. doi:10.1016/j.buildenv.2014.11.028.

[64] C. R. Chu, Y. H. Chiu, Y. T. Tsai, S. L. Wu, Wind-driven natural ventilation for buildings with two openings on the same external wall, Energy and Buildings 108 (2015) 365–372. doi:10.1016/j.enbuild.2015.09.041.

[65] M. Krajčík, A. Simone, B. W. Olesen, Air distribution and ventilation effectiveness in an occupied room heated by warm air, Energy and Buildings 55 (2012) 94–101. doi:10.1016/j.enbuild.2012.08.015.

[66] ASHRAE, Handbook of Fundamentals, 1981, Technical Report, American Society for Heating, Refrigerating, and Air-Conditioning Engineers, Atlanta, GA, 1981.

[67] J. A. Duffie, W. A. Beckman, Solar Engineering of Thermal Processes: Fourth Edition, 4th ed ed., John Wiley, Hoboken, 2013. doi:10.1002/9781118671603.

[68] M. Mirsadeghi, D. Cóstola, B. Blocken, J. L. Hensen, Review of external convective heat transfer coefficient models in building energy simulation programs: Implementation and uncertainty, Applied Thermal Engineering 56 (2013) 134–151. doi:10.1016/j.applthermaleng.2013.03.003.

[69] Lawrence Berkeley Laboratory (LBL), DOE2.1E-053 Source Code, 1994. URL: http://www.doe2.com/.

[70] National Renewable Energy Laboratory, The National Solar Radiation Database NSRDB, 2020. URL: https://nsrdb.nrel.gov/.

[71] G. M. Stavrakakis, M. K. Koukou, M. G. Vrachopoulos, N. C. Markatos,

Natural cross-ventilation in buildings: Building-scale experiments, numerical simulation and thermal comfort evaluation, Energy and Buildings 40 (2008) 1666–1681. doi:10.1016/j.enbuild.2008.02.022.

[72] R. Levinson, H. Akbari, Effects of composition and exposure on the solar reflectance of portland cement concrete, Cement and Concrete Research 32 (2002) 1679–1698. doi:10.1016/S0008-8846(02)00835-9.

[73] F. Collet, L. Serres, J. Miriel, M. Bart, Study of thermal behaviour of clay wall facing south, Building and Environment 41 (2006) 307–315. doi:10.1016/j.buildenv.2005.01.024.

[74] R. Černý, A. Kunca, V. Tydlitát, J. Drchalová, P. Rovnaníková, Effect of pozzolanic admixtures on mechanical, thermal and hygric properties of lime plasters, Construction and Building Materials 20 (2006) 849–857. doi:10.1016/j.conbuildmat.2005.07.002.

[75] Z. Pavlík, A. Trník, M. Keppert, M. Pavlíková, J. Žumár, R. Černý, Experimental investigation of the properties of lime-based plaster containing PCM for enhancing the heat storage capacity of building envelopes, International Journal of Thermophysics 35 (2014) 767–782. doi:10.1007/s10765-013-1550-8.

[76] Z. Pavlík, J. Fořt, M. Pavlíková, J. Pokornỳ, A. Trník, R. Černỳ, Modified lime-cement plasters with enhanced thermal and hygric storage capacity for moderation of interior climate, Energy and Buildings 126 (2016) 113–127. doi:10.1016/j.enbuild.2016.05.004.

[77] K. Dornelles, V. Roriz, M. Roriz, Determination of the solar absorptance of opaque surfaces, Sun, Wind and Architecture - The Proceedings of the 24th International Conference on Passive and Low Energy Architecture, PLEA 2007 3 (2007) 452–459. doi:10.13140/RG.2.1.2368.1764.

[78] K. A. Sabapathy, S. Gedupudi, Straw bale based constructions: Measurement of effective thermal transport properties, Construction and Building Materials 198 (2019) 182–194. doi:10.1016/j.conbuildmat.2018.11.256.

[79] M. Lawrence, A. Heath, P. Walker, The impact of external finishes on the weather resistance of straw bale walls, in: 11th International Conference on Non-conventional Materials and Technologies, NOCMAT 2009, 2009, p. 8.

[80] Q. Chen, J. Srebric, A procedure for verification, validation, and reporting of indoor environment CFD analyses, HVAC and R Research 8 (2002) 201–216. doi:10.1080/10789669.2002.10391437.

[81] E. Rajasekar, A. Ramachandraiah, Adaptive comfort and thermal expectations-a subjective evaluation in hot humid climate, Proceedings of Conference: Adapting to Change: New Thinking on Comfort, WINDSOR 2010 (2010) 9–11.

[82] C. V. Subramanian, N. Ramachandran, S. Senthamil Kumar, Design and Analysis of Solar Passive Architecture for Thermal Comfort of Residential Buildings in Warm-Humid Climate of Thanjavur

Region, Indian Journal of Science and Technology 10 (2017) 1–8. doi:10.17485/ijst/2017/v10i9/103647.

[83] S. Kumar, J. Mathur, S. Mathur, M. K. Singh, V. Loftness, An adaptive approach to define thermal comfort zones on psychrometric chart for naturally ventilated buildings in composite climate of India, Building and Environment 109 (2016) 135–153. doi:10.1016/j.buildenv.2016.09.023.

[84] A. Udaykumar, E. Rajasekar, R. Venkateswaran, Thermal comfort characteristics in naturally ventilated, residential apartments in a hot-dry climate of India, Indoor and Built Environment 24 (2015) 101–115. doi:10.1177/1420326X13504120.

Appendix A. Supplementary data and results

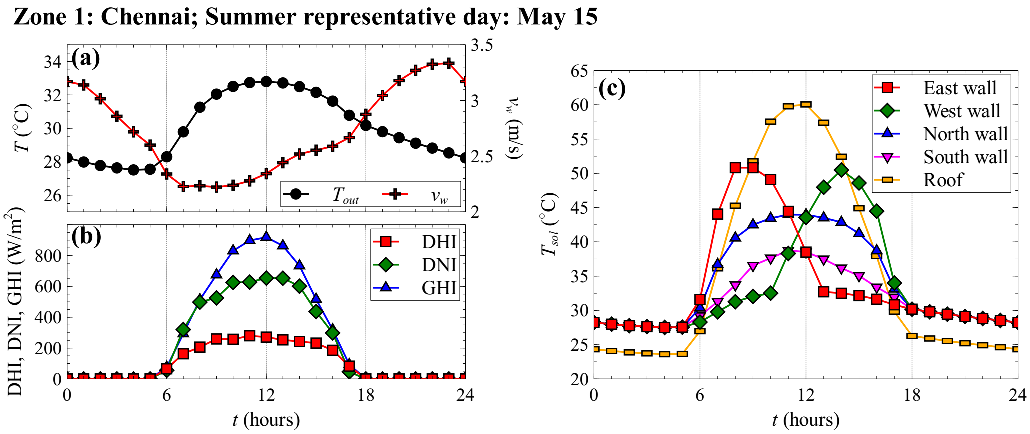

Figure A1: The five-year averaged data for summer of zone 1 used as input in the simulation analysis: (a) Outdoor ambient temperature (T_{out}) and wind speed (V_w), (b) the radiation components, Diffuse Horizontal Irradiance (DHI), Direct Normal Irradiance (DNI) and Global Horizontal Irradiance (GHI) and (c) sol-air temperatures (T_{sol}) calculated for each surface.

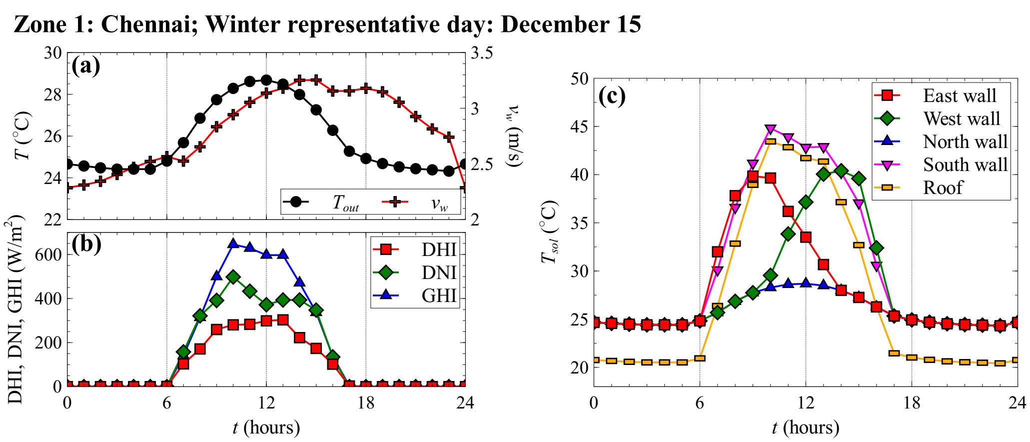

Figure A2: The five-year averaged data for winter of zone 1 used as input in the simulation analysis: (a) Outdoor ambient temperature (T_{out}) and wind speed (V_w), (b) the radiation components, Diffuse Horizontal Irradiance (DHI), Direct Normal Irradiance (DNI) and Global Horizontal Irradiance (GHI) and (c) sol-air temperatures (T_{sol}) calculated for each surface.

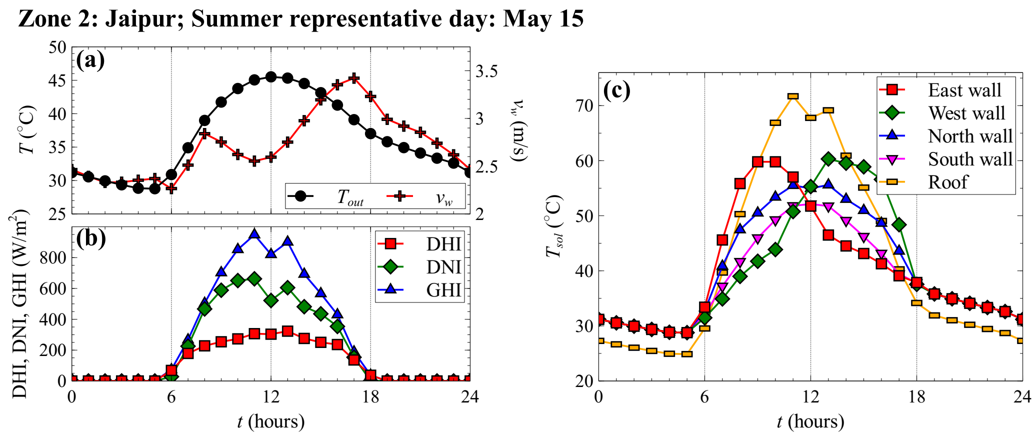

Figure A3: The five-year averaged data for summer of zone 2 used as input in the simulation analysis: (a) (a) Outdoor ambient temperature (T_{out}) and wind speed (V_w), (b) the radiation components, Diffuse Horizontal Irradiance (DHI), Direct Normal Irradiance (DNI) and Global Horizontal Irradiance (GHI) and (c) sol-air temperatures (T_{sol}) calculated for each surface.

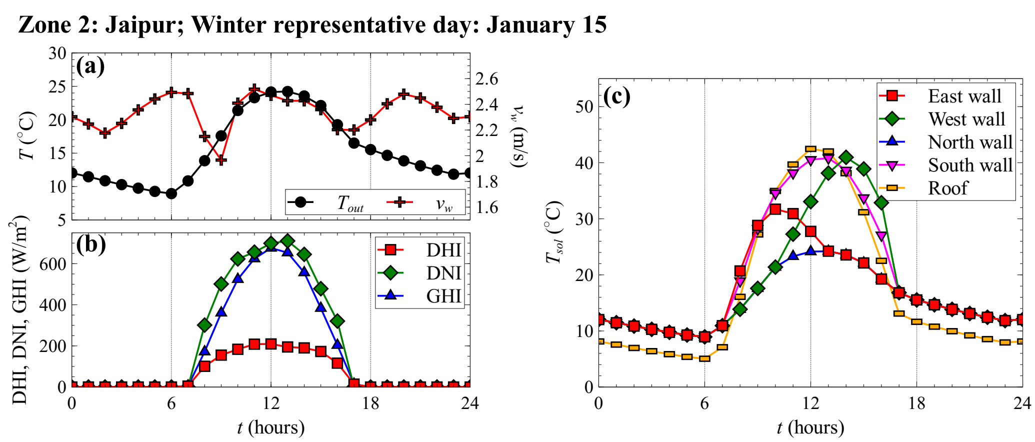

Figure A4: The five-year averaged data for winter of zone 2 used as input in the simulation analysis: (a) Outdoor ambient temperature (T_{out}) and wind speed (V_w), (b) the radiation components, Diffuse Horizontal Irradiance (DHI), Direct Normal Irradiance (DNI) and Global Horizontal Irradiance (GHI) and (c) sol-air temperatures (T_{sol}) calculated for each surface.

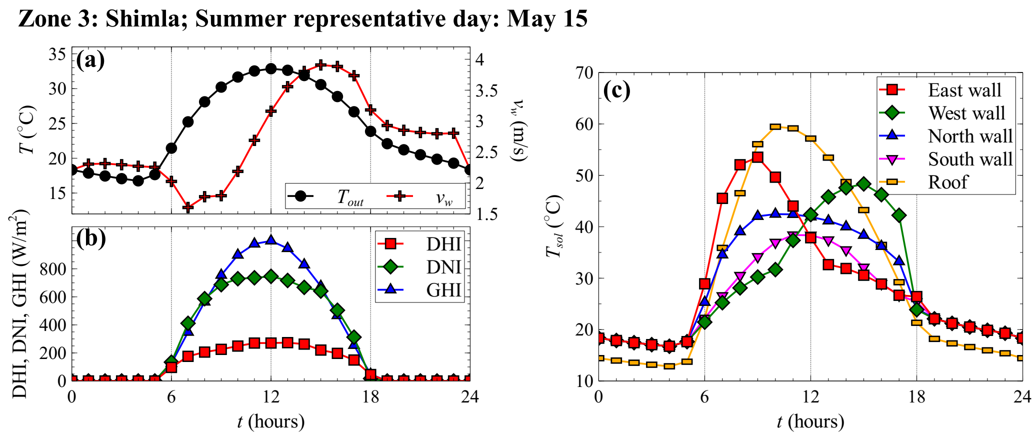

Figure A5: The five-year averaged data for summer of zone 3 used as input in the simulation analysis: (a) Outdoor ambient temperature (T_{out}) and wind speed (V_w), (b) the radiation components, Diffuse Horizontal Irradiance (DHI), Direct Normal Irradiance (DNI) and Global Horizontal Irradiance (GHI) and (c) sol-air temperatures (T_{sol}) calculated for each surface.

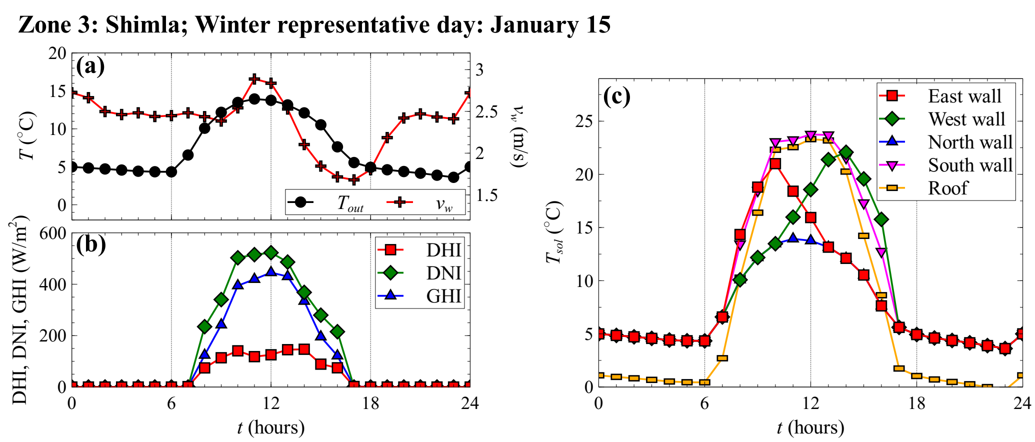

Figure A6: The five-year averaged data for winter of zone 3 used as input in the simulation analysis: (a) Outdoor ambient temperature (T_{out}) and wind speed (V_w), (b) the radiation components, Diffuse Horizontal Irradiance (DHI), Direct Normal Irradiance (DNI) and Global Horizontal Irradiance (GHI) and (c) sol-air temperatures (T_{sol}) calculated for each surface.

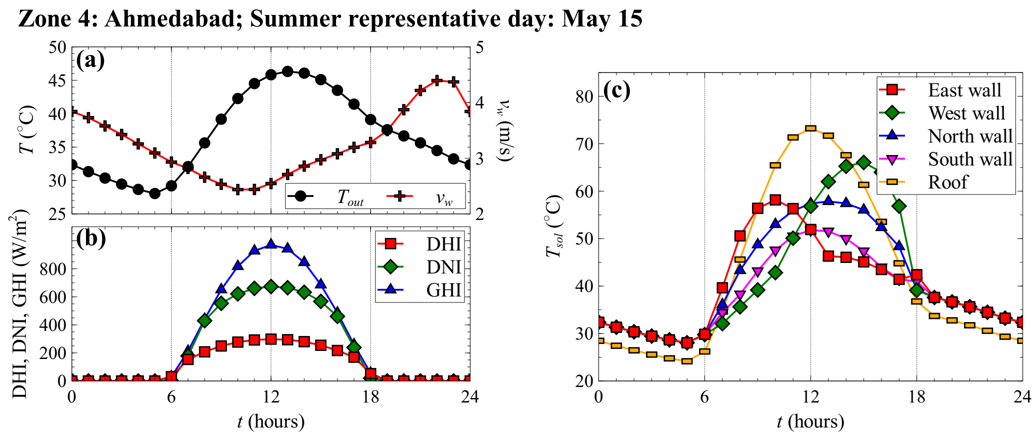

Figure A7: The five-year averaged data for summer of zone 4 used as input in the simulation analysis: (a) Outdoor ambient temperature (T_{out}) and wind speed (V_w), (b) the radiation components, Diffuse Horizontal Irradiance (DHI), Direct Normal Irradiance (DNI) and Global Horizontal Irradiance (GHI) and (c) sol-air temperatures (T_{sol}) calculated for each surface.

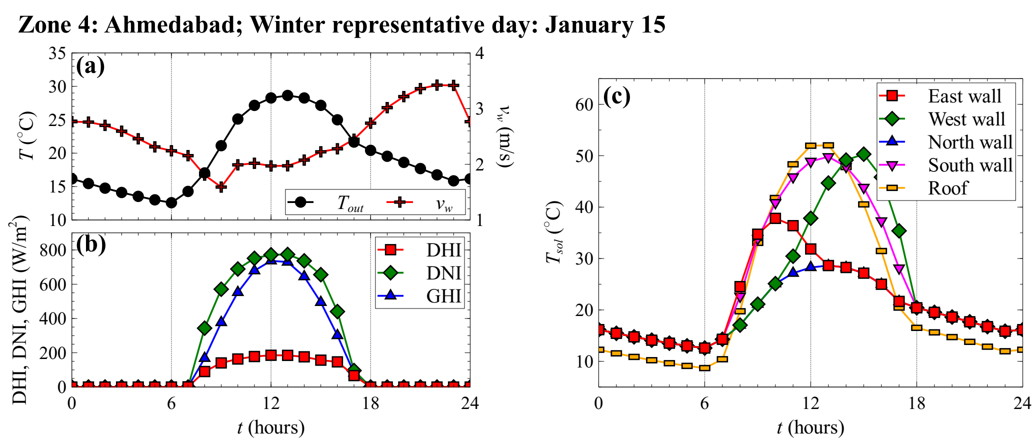

Figure A8: The five-year averaged data for winter of zone 4 used as input in the simulation analysis: (a) Outdoor ambient temperature (T_{out}) and wind speed (V_w), (b) the radiation components, Diffuse Horizontal Irradiance (DHI), Direct Normal Irradiance (DNI) and Global Horizontal Irradiance (GHI) and (c) sol-air temperatures (T_{sol}) calculated for each surface.

Zone 5: Bengaluru; Summer representative day: April 15

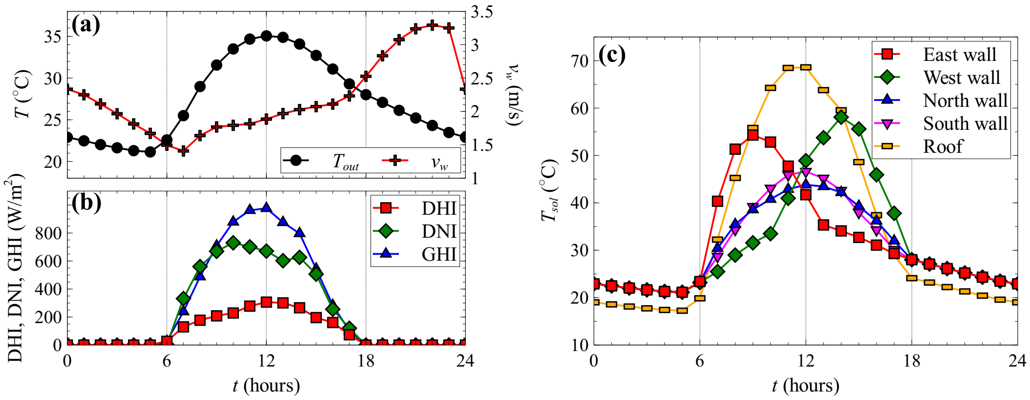

Figure A9: The five-year averaged data for summer of zone 5 used as input in the simulation analysis: (a) Outdoor ambient temperature (T_{out}) and wind speed (V_w), (b) the radiation components, Diffuse Horizontal Irradiance (DHI), Direct Normal Irradiance (DNI) and Global Horizontal Irradiance (GHI) and (c) sol-air temperatures (T_{sol}) calculated for each surface.

Zone 5: Bengaluru; Winter representative day: December 15

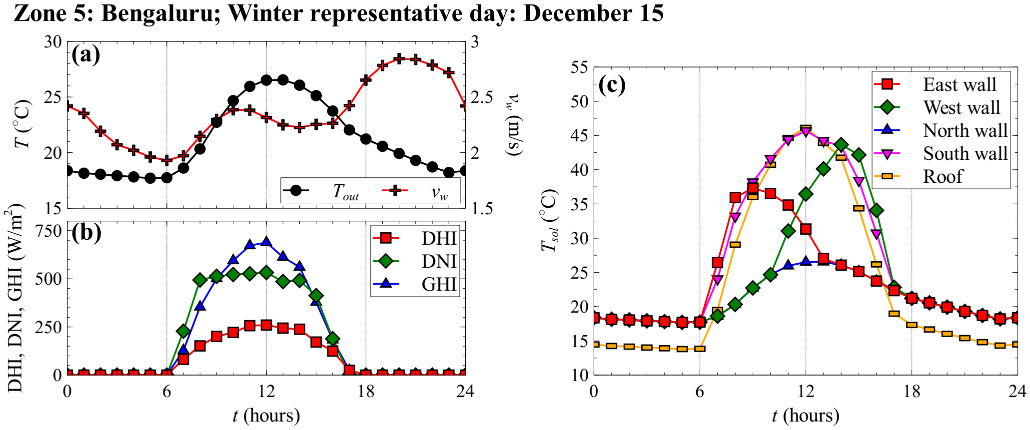

Figure A10: The five-year averaged data for winter of zone 5 used as input in the simulation analysis: (a) Outdoor ambient temperature (T_{out}) and wind speed (V_w), (b) the radiation components, Diffuse Horizontal Irradiance (DHI), Direct Normal Irradiance (DNI) and Global Horizontal Irradiance (GHI) and (c) sol-air temperatures (T_{sol}) calculated for each surface.